

AD-A175 246

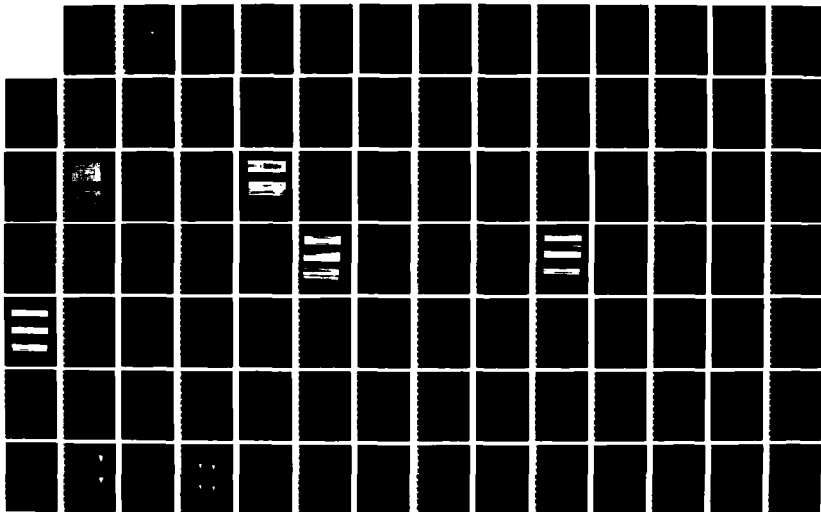
NUCLEATE POOL-BOILING OF R-114 REFRIGERANT AND OIL
MIXTURES FROM WATER-HEATED ENHANCED SURFACES(U) NAVAL
POSTGRADUATE SCHOOL MONTEREY CA S M MCMAHUS JUN 86

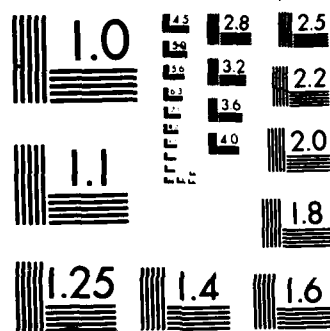
1/2

UNCLASSIFIED

F/G 20/13

NL





PHOTOCOPY RESOLUTION TEST CHART

(2)

NAVAL POSTGRADUATE SCHOOL

Monterey, California

AD-A175 246



DTIC
DEC 16 1986

THESIS

NUCLEATE POOL-BOILING
OF R-114 REFRIGERANT AND OIL MIXTURES
FROM WATER-HEATED ENHANCED SURFACES

by

Stephen M. McManus

June 1986

Thesis Advisor:
Co-Advisor:

P. J. Marto
A. S. Wanniarachchi

DTIC FILE COPY

Approved for public release; distribution unlimited.

86 11 19 042

DISCLAIMER NOTICE

**THIS DOCUMENT IS BEST QUALITY
PRACTICABLE. THE COPY FURNISHED
TO DTIC CONTAINED A SIGNIFICANT
NUMBER OF PAGES WHICH DO NOT
REPRODUCE LEGIBLY.**

AD-A175-246

REPORT DOCUMENTATION PAGE

1a REPORT SECURITY CLASSIFICATION UNCLASSIFIED		1b. RESTRICTIVE MARKINGS	
2a SECURITY CLASSIFICATION AUTHORITY		3 DISTRIBUTION/AVAILABILITY OF REPORT Approved for public release; distribution unlimited.	
2b DECLASSIFICATION/DOWNGRADING SCHEDULE		5 MONITORING ORGANIZATION REPORT NUMBER(S)	
4 PERFORMING ORGANIZATION REPORT NUMBER(S)		7a. NAME OF MONITORING ORGANIZATION Naval Postgraduate School	
6a NAME OF PERFORMING ORGANIZATION Naval Postgraduate School	6b OFFICE SYMBOL (If applicable) Code 69	7b. ADDRESS (City, State, and ZIP Code) Monterey, California 93943-5000	
8a NAME OF FUNDING/SPONSORING ORGANIZATION David W. Taylor NSRDC	8b OFFICE SYMBOL (If applicable)	9 PROCUREMENT INSTRUMENT IDENTIFICATION NUMBER	
8c ADDRESS (City, State, and ZIP Code) Annapolis, Maryland 21402		10 SOURCE OF FUNDING NUMBERS PROGRAM ELEMENT NO PROJECT NO TASK NO WORK UNIT ACCESSION NO	
11 TITLE (Include Security Classification) Nucleate Pool-Boiling of R-114 Refrigerant and Oil Mixtures from Water-Heated Enhanced Surfaces			
12 PERSONAL AUTHOR(S) McManus, Stephen, M.			
13a TYPE OF REPORT Master's Thesis	13b TIME COVERED FROM TO	14 DATE OF REPORT (Year, Month, Day) 1986, June	15 PAGE COUNT 99
16 SUPPLEMENTARY NOTATION			
17 COSATI CODES FIELD GROUP SUB-GROUP		18 SUBJECT TERMS (Continue on reverse if necessary and identify by block number) Nucleate Pool-Boiling; Water-Heated Tubes; Enhanced Surfaces; Theses; Computer Programs. G	
19 ABSTRACT (Continue on reverse if necessary and identify by block number) Heat-transfer measurements were made for a single, water-heated tube in a pool of R-114 to simulate operating conditions of a water chiller. Data were obtained for a smooth copper tube, and for two commercially available tubes: a spirally roped copper/nickel tube with a porous coating; and a copper tube with a structured outer surface and a multiple-start helical ridged inner surface. Measurements were made for refrigerant/oil mixtures at oil concentrations from 0 to 6 mass percent with a boiling pool temperature of 15.8 °C. Results for the two enhanced tubes with and without oil are compared to the smooth tube data. Enhancement factors for the overall heat-transfer coefficient were 4.0 and 3.6 for the structured surface and porous-coated tubes, respectively, in pure refrigerant and at a water velocity of 2 m/s. For these same conditions the enhancement factors (cont. next page)			
20 DISTRIBUTION AVAILABILITY OF ABSTRACT UNCLASSIFIED UNLIMITED <input type="checkbox"/> SAME AS RPT <input type="checkbox"/> DTIC USERS		21 ABSTRACT SECURITY CLASSIFICATION Unclassified	
22a RESPONSIBLE INDIVIDUAL J. J. MCGLOTHLIN		22b TELEPHONE (Include Area Code) (408) 646-2586	22c OFFICE SYMBOL 69 MX

Unclassified

SECURITY CLASSIFICATION OF THIS PAGE (When Data Entered)

19. (cont)

for the out-side heat-transfer coefficient were 14.6 and 6.4 for the porous-coated and structured surface tubes, respectively.

NO 102-15014-6601

Unclassified

SECURITY CLASSIFICATION OF THIS PAGE(When Data Entered)

Approved for public release; distribution is unlimited.

Nucleate Pool-Boiling
of R-114 Refrigerant and Oil Mixtures
from Water-Heated Enhanced Surfaces

by

Stephen M. McManus
Lieutenant, United States Navy
B.S.Ch.E., University of New Mexico, 1979

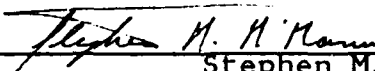
Submitted in partial fulfillment of the
requirements for the degree of

MASTER OF SCIENCE IN MECHANICAL ENGINEERING


from the

NAVAL POSTGRADUATE SCHOOL
June 1986

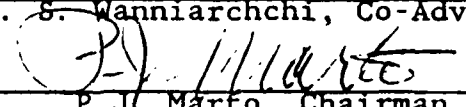
Author:

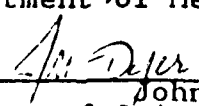

Stephen M. McManus

Approved by:


P.J. Marto, Thesis Advisor


A. S. Wanniarachchi, Co-Advisor


P.J. Marto, Chairman,
Department of Mechanical Engineering


John N. Dyer,
Dean of Science and Engineering

ABSTRACT

Heat-transfer measurements were made for a single, water-heated tube in a pool of R-114 to simulate operating conditions of a water chiller. Data were obtained for a smooth copper tube, and for two commercially available tubes: a spirally roped copper-nickel tube with a porous coating; and a copper tube with a structured outer surface and a multiple-start helical ridged inner surface. Measurements were made for refrigerant-oil mixtures at oil concentrations from 0 to 6 mass percent with a boiling pool temperature of 13.8 °C. Results for the two enhanced tubes with and without oil are compared to the smooth tube data. Enhancement factors for the overall heat-transfer coefficient were 4.0 and 3.6 for the structured surface and porous-coated tubes, respectively, in pure refrigerant and at a water velocity of 2 m/s. For these same conditions the enhancement factors for the outside heat-transfer coefficient were 14.6 and 6.4 for the porous-coated and structured surface tubes, respectively.

TABLE OF CONTENTS

I.	INTRODUCTION	11
II.	BACKGROUND	14
	A. NUCLEATE BOILING	14
	B. EXTERNAL SURFACE ENHANCEMENT	14
	C. EFFECTS OF OIL	20
	D. INTERNAL ENHANCEMENT	21
III.	EXPERIMENTAL APPARATUS	24
	A. OVERALL APPARATUS	24
	B. BOILING TUBE CONSTRUCTION	27
	C. COMPUTER-CONTROLLED DATA ACQUISITION AND REDUCTION	30
IV.	EXPERIMENTAL PROCEDURES	32
	A. FLOWMETER CALIBRATION	32
	B. BOILING TUBE AND APPARATUS PREPARATION	32
	C. BOILING DATA RUNS	34
	D. DATA ACQUISITION AND REDUCTION	36
V.	RESULTS AND DISCUSSION	38
	A. INSIDE HEAT-TRANSFER COEFFICIENT	38
	B. LIGHT OFF EFFECTS	41
	C. SMOOTH TUBE	43
	D. HIGH FLUX TUBE	46
	E. TURBO-B TUBE	51
	F. COMPARISON OF BOILING HEAT-TRANSFER COEFFICIENTS	51
	G. OVERALL HEAT-TRANSFER CHARACTERISTICS	56
VI.	CONCLUSIONS AND RECOMMENDATIONS	58
	A. CONCLUSIONS	58

B. RECOMMENDATIONS	58
APPENDIX A: DATA REDUCTION PROGRAM	60
APPENDIX B: FLOWMETER CALIBRATION	80
APPENDIX C: MODIFIED WILSON PLOT	85
APPENDIX D: DATA RUNS	88
APPENDIX E: UNCERTAINTY ANALYSIS	91
APPENDIX F: LIST OF NOMENCLATURE	93
1. NOMENCLATURE	93
2. SUBSCRIPTS	94
LIST OF REFERENCES	95
INITIAL DISTRIBUTION LIST	98

LIST OF TABLES

1.	CHANNEL DESIGNATIONS	31
2.	BOILING RUN REPEATABILITY	35
3.	DRP4 MAJOR SECTIONS	61
4.	DATA RUN DESCRIPTION	89
5.	UNCERTAINTY ANALYSIS PERCENTS	92

LIST OF FIGURES

2.1	Schematic of Porous Coating (from Ref. 8).	16
2.2	Schematic of Manufactured Reentrant Cavity (from Ref. 8)	17
2.3	Physical Model of Bubble Mechanism (from Ref. 15)	19
2.4	Physical Model of Oil Effect on Bubble Formation (from Ref. 16)	22
3.1	Schematic of Experimental Apparatus	25
3.2	Photographs of Experimental Apparatus.	26
3.3	Schematic of Boiling Tubes	28
	(A) Smooth Tube	28
	(B) Korodense Tube With High Flux Coating	28
	(C) Turbo-B Tube	28
3.4	Photographs of Internal Enhancement	29
	(A) Korodense Tube	29
	(B) Turbo-B Tube	29
5.1	Variation of Heat Flux with Wall Superheat at 0% Oil.	39
5.2	Light Off Effect at 0% Oil	42
5.3	Steam Initiation	44
	(A) for Smooth Tube	44
	(B) for High Flux Tube	44
	(C) for Turbo-B Tube	44
5.4	Variation of Heat Flux with Wall Superheat for Smooth Tube	45

5.5	Variation of Heat Flux with Wall Superheat for High Flux Tube	47
5.6	Boiling from High Flux Surface	48
	(A) at 0% Oil	48
	(B) at 2% Oil	48
	(C) at 6% Oil	48
5.7	Variation of Heat Flux with Changing Water Inlet Temperature for High Flux Tube	50
5.8	Variation of Heat Flux with Wall Superheat for Turbo-B Tube	52
5.9	Boiling from Turbo-B Surface	53
	(A) at 0% Oil	53
	(B) at 2% Oil	53
	(C) at 6% Oil	53
5.10	Variation of Heat Flux with Changing Water Inlet Temperature for Turbo-B Tube	54
5.11	Variation of Overall Heat-Transfer Coefficient with Oil Mass Percent	55
5.12	Variation of Boiling Heat-Transfer Ratio at a Heat Flux of 40 kW/m^2	57
B.1	Effect of Float Shape on Coefficient of Discharge	82
	(A) Square Edge Plumb Bob Float (from Ref. 31)	82
	(B) Taper Edge Plumb Bob Float	82
B.2	Effect of Float Shape on Streamline Pattern	84
	(A) Square Edge Plumb Bob Float (from Ref. 31)	84
	(B) Taper Edge Plumb Bob Float	84

ACKNOWLEDGEMENTS

The author wishes to express his appreciation to Dr. Paul J. Marto and Dr. A. S. Wanniararchchi for their advice, guidance, and enthusiastic support towards the completion of this thesis.

The author also expresses his sincere gratitude to his wife, Kay, and children, Alicia and James, for their patience with the long hours and frustrations inherent in such an endeavor.

I. INTRODUCTION

Recent developments in boiling surfaces have shown considerable enhancements in heat transfer performance. The worldwide literature on enhanced heat transfer contains over 3000 published technical papers and reports [Ref. 1: p. 81]. This increased interest in heat transfer augmentation is the result of incentives for energy and material savings. One effective way to improve the heat transfer is by using passive augmentation.

Passive augmentation uses fine-scale alteration of surfaces, both external and internal [Ref. 1: p. 82]. These surfaces may consist of either an applied porous coating or fins deformed in various ways to provide a large number of reentrant cavities on external surfaces. Methods of internal enhancement include insert devices, forged fins, or deformation of the surface (i.e., spirally roped or corrugated tube). The use of such surfaces can lead to considerable reduction in the size and weight of heat-transfer equipment. The reductions may lead to smaller capital costs or operating costs or both.

Of particular interest, in naval applications, is the reduction in the size of water chillers in refrigeration systems. While a number of investigations are currently in progress, the theoretical treatment of the boiling performance of various tubes is almost impossible owing to the very complicated mechanisms involved. The degree of difficulty increases with the presence of oil in the refrigerant liquid. In general, refrigeration systems with oil-lubricated, hermetically sealed compressors contain small mass percents of oil in the refrigerant liquid. Therefore, reliable data covering a wide variety of operating conditions for various refrigerants and different boiling

surfaces is essential to further develop more compact and efficient evaporators.

Most of the experiments on enhanced boiling surfaces reported in the literature have used electrically heated tubes. The difficulties associated with these tubes, especially during the instrumentation stage, raise questions as to the reliability of the data as described by Wanniarachchi et al [Ref. 2: p. 14]. Despite the precautions taken to minimize contact resistance, it may still be present between the thermocouple locations and the outer boiling surface. Another area of doubt, described by Wanniarachchi et al. [Ref. 2: p. 14], is the nonuniform heat fluxes generated by commercially available electrical heaters. Additionally, in order to use an electrical heated tube, the inside surface of the tube must be smooth, or any internal enhancement must be bored out. This is disadvantageous as designers would be interested in knowing the overall heat-transfer coefficient. Most industrial experiments use 2-to 3-meter-long tubes with warm water flowing inside them. While the information generated from these experiments closely approximate actual evaporators, compared to electrical heated tubes, the large water temperature drop from inlet to exit (up to 5 K) may make it difficult to study the details of the boiling process.

The type of refrigerant selected will also influence the design of evaporators. R-114, a moderate-pressure refrigerant, is receiving more attention, in particular for naval applications. Advantages to using R-114 include: (a) it belongs to the refrigerant group with the lowest toxicity, (b) it is very stable with temperature, and (c) it has a fairly large value for the energy transfer per unit volume of vapor (i.e., $E_v = h_{fg} / v_g$) [Ref. 3: pp. 281-291]. The advantages of the first two items are clear. The third item is advantageous since a higher value for E_v means lower

pressure drop through the refrigerant piping for a specified heat duty. As the normal boiling point of the type of refrigerant increases, the E_v value increases. R-11, R-113, R-114, and R-22 have E_v values in increasing order. R-114 may be preferable to R-11 and R-113 due to the higher E_v value and preferable to R-22 due to the ability to use lighter components in the refrigeration loop.

Based on the above discussion, the major objective of the present investigation was to study the boiling performance of two commercially available tubes, a porous-coated tube and a mechanically structured surface, in comparison with a smooth tube for the following conditions: (a) tubes are water-heated, (b) boiling fluid is R-114 with 0, 1, 2, and 6 percent by mass oil, and (c) boiling temperature is 13.8 °C.

II. BACKGROUND

A. NUCLEATE BOILING

When the temperature of a boiling surface exceeds the saturation temperature of a fluid by a few degrees, nucleate boiling occurs. The difference between the boiling surface and saturation temperature is the amount of wall superheat. Dougherty [Ref. 4: p. 175] defined pool-boiling as vaporization occurring under the following conditions: (1) liquid depth \gg the bubble diameter, (2) there is negligible effect on heat transfer due to low or no externally imposed velocity of the fluid, and (3) the bubbles move away from the boiling surface due to a force field. With the above conditions, the heat flow can be expressed as:

$$h = \frac{Q}{A\Delta T} \quad (2.1)$$

A description of the boiling mechanism is given by Chongrungreong and Sauer [Ref. 5: p. 701]. A thin layer of superheated liquid is formed adjacent to the boiling surface. Bubbles nucleate in this thin layer and grow from preferred spots on the boiling surface. It is assumed that the primary resistance to heat transfer is within the thin liquid layer. The height of the liquid in the boiling container is not a primary variable, but the liquid properties should be controlled. However, large flooded evaporators may experience a significant "submergence effect" from the liquid head.

B. EXTERNAL SURFACE ENHANCEMENT

For smooth heating surfaces, bubbles nucleate at various scratches and cavities on the surface. Fujii stated that the number of active sites increases as the heat flux increases

[Ref. 6: p. 48]. Webb [Ref. 7: p. 46] stated that the ability to enhance the nucleate boiling coefficient by applying some type of roughness has been known for over 50 years.

Presently, there are two major types of commercially developed roughnesses: (1) porous coating and (2) various fins and surfaces with reentrant cavities [Ref. 8: p. 24]. The first type of roughness is a sintered particle coating, usually copper or aluminum. Figure 2.1 shows a schematic and a photomicrograph of a porous coating. The small reentrant cavities are interconnected by substrate tunnels. The surface reduces the required superheat for vapor generation by entrapping a high density of relatively large vapor nuclei in the cavities contained within the porous coating [Ref. 8: p. 24]. As described by Webb [Ref. 7: p. 58], researchers found that a critical pore size not a particle size governs the number of nucleation sites. Large pores are required for liquids with high surface tension and high thermal conductivity, while small pores work best for liquids with low surface tension and low thermal conductivity (i.e., refrigerants). Czikk and O'Neill [Ref. 9: p. 53] developed correlations to include the effects of different pore sizes of porous-coatings. They concluded that there were two resistances to heat transfer for these coatings: a nucleation superheat related to bubble diameter; and a conduction superheat controlled by the liquid film separating the vapor bubbles from the metal matrix. Carnavos [Ref. 10: pp. 106-108] found that a porous coating resulted in a 700-800 percent better heat-transfer coefficient than a smooth surface in a pool of R-11. Czikk [Ref. 11: p. 98] also found increased performance of the porous-coated tubes used in his 20-ton water-chiller experiment.

Structured fins or surfaces form reentrant cavities of various geometries. Figure 2.2 is shows an example of a

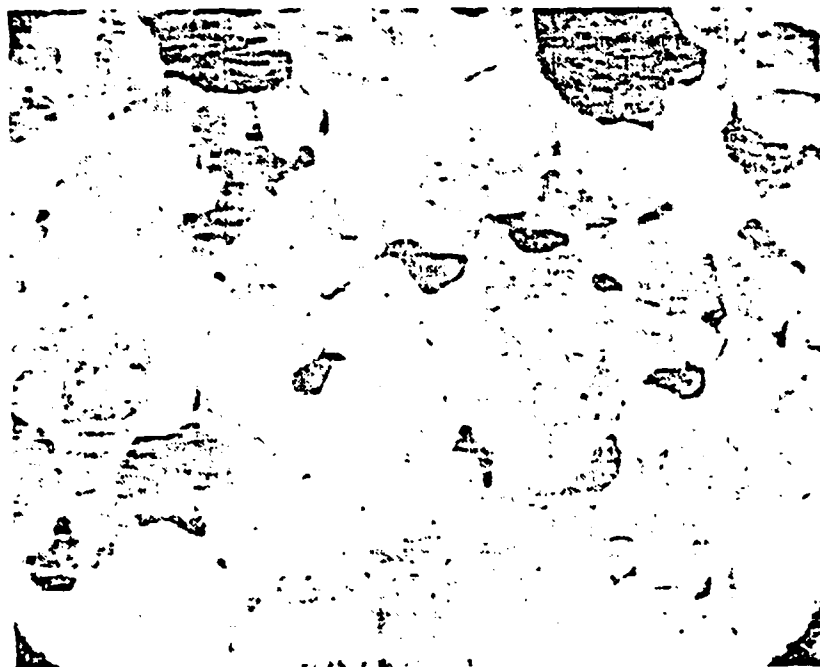
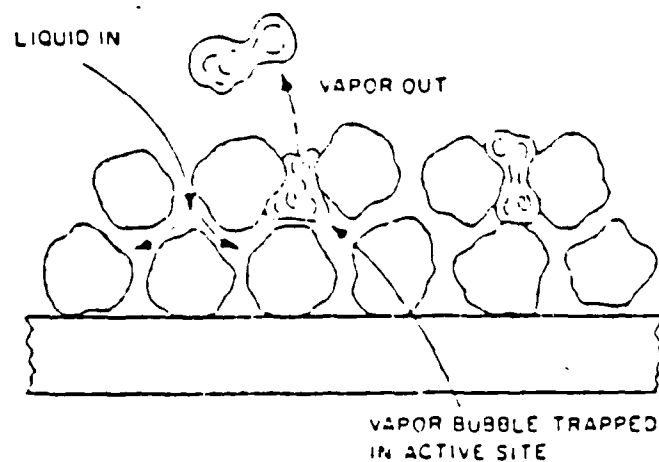


Figure 2.1. Schematic and Scanning Electron Micrograph (500x) of High Flux Surface (from Ref. 8).

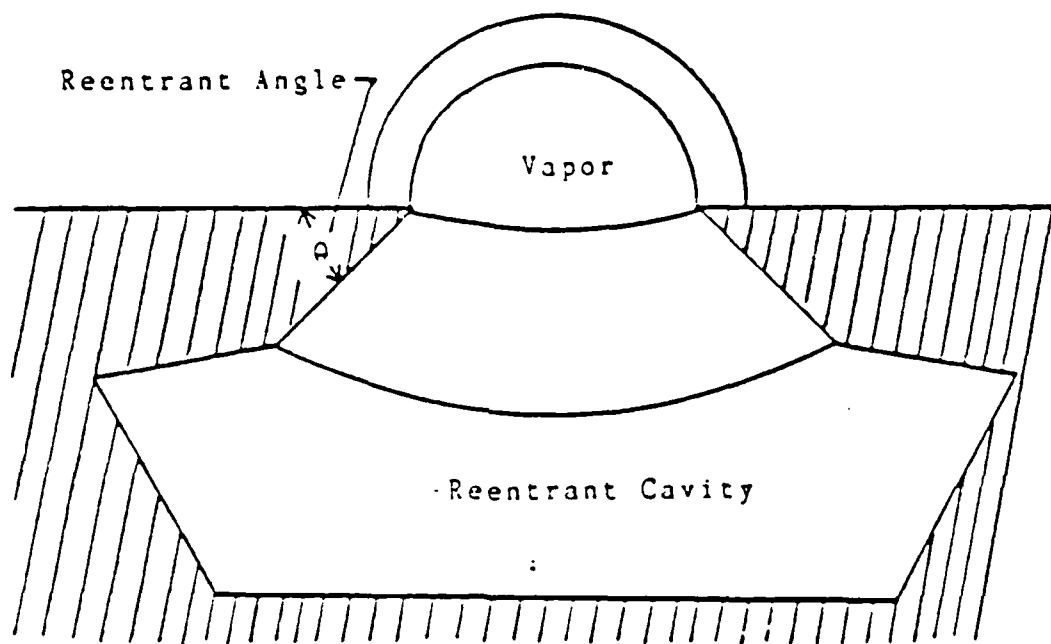


Figure 2.2. Schematic of Manufactured Reentrant Cavity
(from Ref. 3).

manufactured reentrant cavity. These reentrant cavities act as stable nucleation sites, which enhances the heat transfer. The nucleation site, to remain active, is dependent on the mouth diameter falling within a critical range and shape with a maximum reentrant angle. This range is a function of the fluid properties. The cost of these surfaces, presently, are not significantly higher than the cost for smooth tubes and they dramatically improve boiling performance compared to the smooth tubes.

The mechanisms by which the reentrant cavities operate are complicated. Previous research concluded that the combination of bubble evaporation, thermal boundary-layer stripping and bubble agitation controlled the heat transfer from smooth surfaces [Ref. 12: p. 192]. In contrast, different experiments conducted by Arshad [Ref. 12: p. 192] and Arai [Ref. 13: p. 37] show that thin film evaporation in the reentrant cavity controlled the heat-transfer mechanism. Bubbles were formed by vapor exiting cavities as the liquid-vapor interface of the thin film contacted the cavity surface. Surface tension holds most of the liquid on the cavity walls. Ayub [Ref. 14: p. 64] showed this similar "thermosiphon mechanism" with his experiments using enhanced surfaces.

Nakayama [Ref. 15: p. 37] gives a fairly detailed description of a physical model undergoing this bubble growth mechanism. Figure 2.3 shows the three major phases of bubble growth. Phase I consists of a pressure buildup in the tunnel by evaporation of liquid held in corners and continues until the meniscus reaches a hemispherical shape of radius $r_0 = d_0/2$ (where d_0 is the mouth diameter of the reentrant cavity). In Phase II, the meniscus grows faster at some pores than at others. The Phase I pressure buildup is reduced as the vapor enters the growing bubbles. The meniscus at inactive pores does not grow due to this vapor

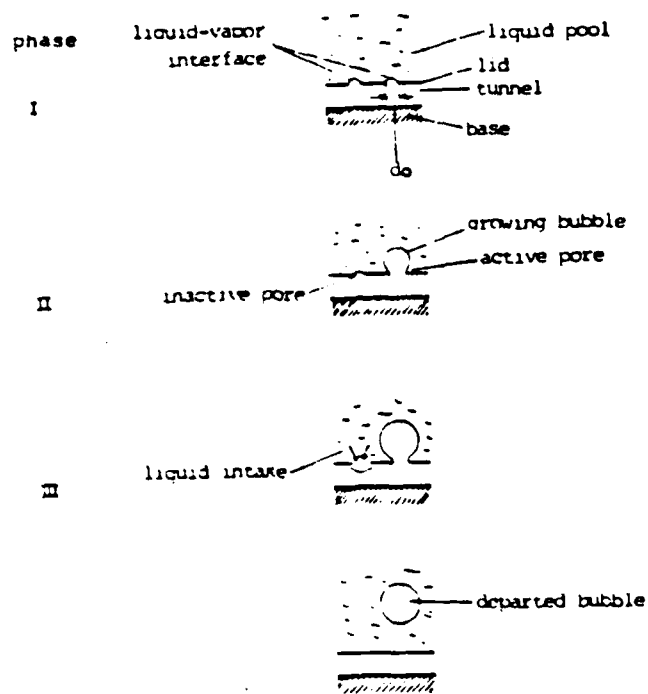


Figure 2.3. Physical Model of Bubble Mechanism (from Ref. 15).

pressure reduction. Initially, the bubble expands under the high internal pressure, while later expansion is controlled by the receding liquid inertia around the bubble. Phase III is termed the liquid intake phase with liquid flowing into the tunnel through inactive pores. This flow is over a short interval of pressure depression which occurs as the pressure of the bubble and tunnel is lower than the pool pressure. The bubble leaves the pore and new meniscus formation closes off the pore, ending this phase and returning the cycle to Phase I.

C. EFFECTS OF OIL

The introduction of oil into the pure refrigerant, in general, causes a decrease in the boiling coefficient as the oil concentration increases. The effects of oil on the mixture are theoretically complicated as most empirical equations relating physical properties are derived from experimental data and not from theoretical equations. Various empirical equations are cited by Chongrungreong and Sauer [Ref. 5: pp. 703-705]. Yet, Jensen and Jackman [Ref. 16: p. 184] showed that the correlation developed by Chongrungreong and Sauer appeared to overpredict as oil concentrations increased due to poor prediction of the mixture viscosity.

Predictive equations were developed by Jensen and Jackman [Ref. 16: pp. 186-187] for density, viscosity, surface tension and specific heat for pure R-113, pure oil, and R-113-oil mixtures. These equations are:

$$\frac{1}{\rho_m} = \frac{C_c}{\rho_{ol}} + \frac{1-C_c}{\rho_{rl}} \quad (2.2)$$

$$\mu_m = \mu_r \exp \left[C_c \left(\frac{\mu_o}{\mu_r} \right)^{0.3} \right] \quad (2.3)$$

$$\sigma_m = \sigma_r + (\sigma_o - \sigma_r) C_c^{0.5} \quad (2.4)$$

$$c_{pm} = (1 - C_c) c_{prl} + c_{pol} \quad (2.5)$$

These equations are based on a physical model shown in Figure 2.4 developed by Jensen and Jackman [Ref. 16: pp. 187-188]. The model shows a bubble growing on a heated surface as the refrigerant evaporates from the superheated liquid phase into the bubble interior. Due to the less volatile nature of the oil in the mixture, it does not evaporate into the bubble, but, remains at the liquid-vapor interface. The decrease in the rate of bubble growth is due to the decrease of oil diffusion into the liquid mixture and the decrease of refrigerant through the oil layer into the bubble. The decrease of the bubble growth rate decreases the heat-transfer rate.

D. INTERNAL ENHANCEMENT

Internal enhancement increases the heat-transfer area, creates additional turbulence, and produces secondary flows, all of which contribute to the increase in the heat transfer. The laminar sublayer is assumed to be the principal resistance to heat transfer [Ref. 17: p. 6]. The developed secondary flow thins the sublayer and moves it into the stream where turbulence prevails and without an increase in shear; likewise, heat transfer is increased without an increase in friction [Ref. 18: p. 30]. Most studies show that the friction factor does increase with internal enhancement but the amount is strongly dependent on the internal enhancement geometry. The increase of both the friction and heat transfer is dependent on fin or rib pitch, groove depths, and helix angles [Refs. 17,19: pp. 6, 19-21]. Additionally, these studies have shown that there are

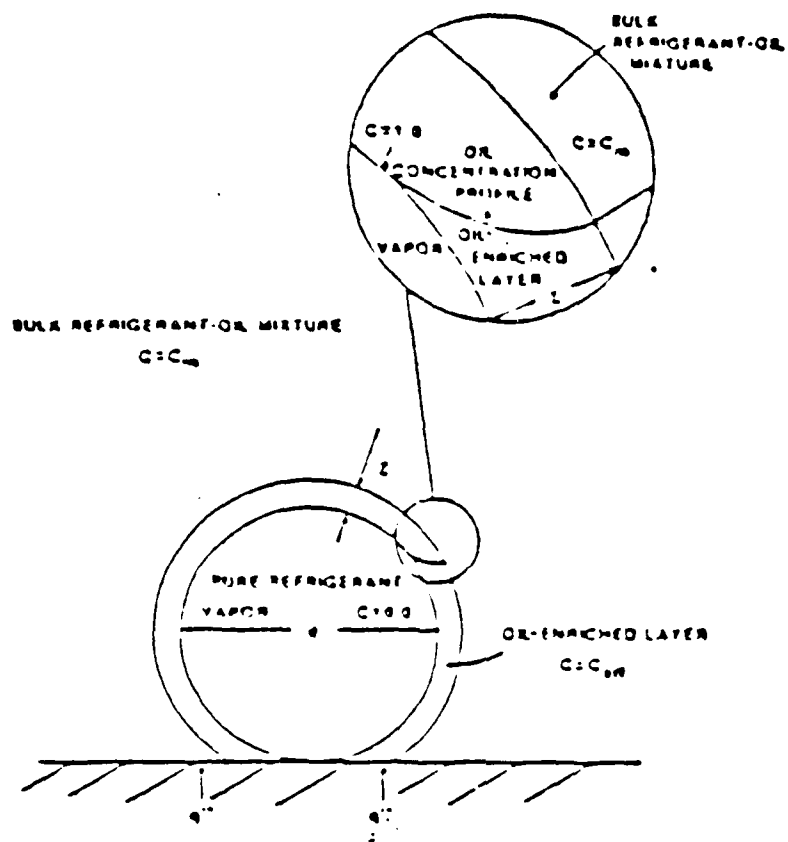


Figure 2.4. Idealized Model of Bubble Growth in Refrigerant-Oil Mixture (from Ref. 16).

critical geometrical dimensions that give the maximum heat transfer. For example, short fins (\ll tube diameter) with rifling will raise heat-transfer coefficients with no problems of flow stagnation. Yet, medium fins may develop flow stagnation and decrease heat-transfer coefficients [Ref. 19: pp. 22-23]. As such, the selection of internal enhancement will generally improve the performance of boiling surfaces.

III. EXPERIMENTAL APPARATUS

A. OVERALL APPARATUS

A schematic of the experimental apparatus is given in Figure 3.1. The photographs in Figure 3.2 show two different views of the apparatus. Complete details on the design and construction of the refrigerant and oil components are given by Karasbun [Ref. 20: pp. 24-32]. A discussion of the modifications for the water heating mode is provided in this paper. The major components of the apparatus are: two Pyrex glass tees, an R-114 liquid reservoir, a water-ethylene glycol mixture sump, an R-12 refrigeration system, a vacuum pump, a water supply tank, three centrifugal pumps, a flow meter, three heaters, a graduated oil cylinder, and an oil reservoir. The R-114 boiling and condensation occurred in the lower and upper glass tees, respectively. The R-114 vapor was condensed by the water-ethylene glycol mixture pumped through a copper condenser coil located in the upper glass tee. A 1/2-Ton R-12 refrigeration system maintained the water-ethylene glycol mixture between -18 and -14 °C.

The major difference between the experimental apparatus used by Karasabun and Reilly [Refs. 20,8: pp. 24-32, 30-35], and the one used during the present investigation concerned the use of water heating instead of electric heating as a means to provide heat to the boiling tube. Filtered tap water supplied from a storage tank (15), was pumped by two 1/2-hp motors (13 and 14) connected in series. A three-way valve (V-16) was provided on the downstream side of the second pump to obtain two flow paths. The normal flow path for data runs was through: the metering valve (V-17), the flowmeter (6), the inlet mixing chamber (16), the boiling tube, the outlet mixing chamber (16), the chambers provided

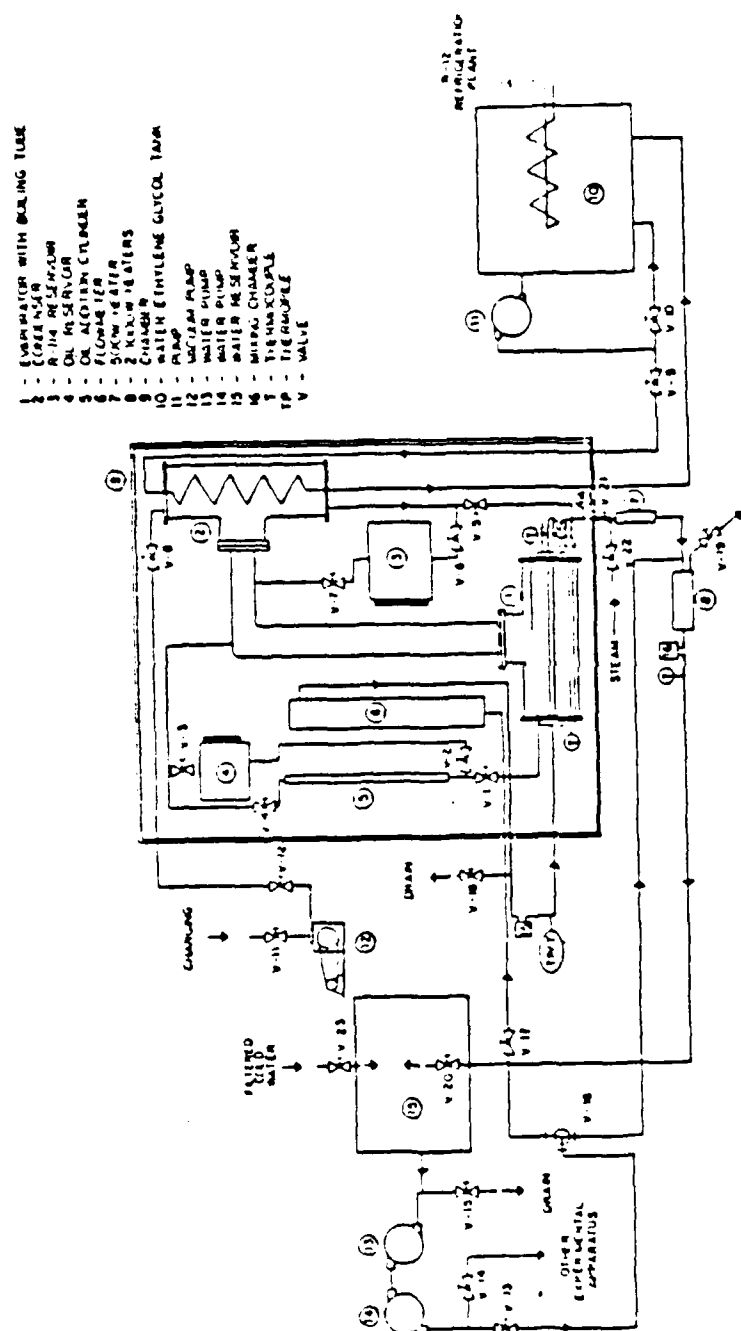
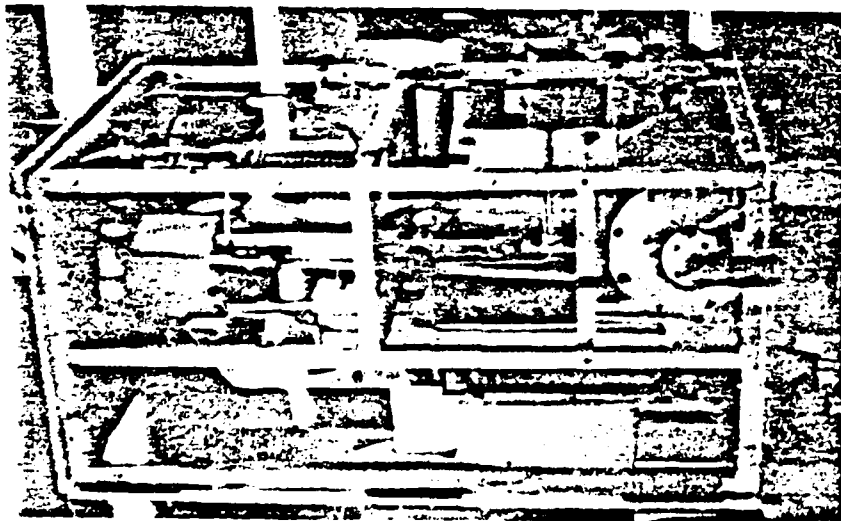
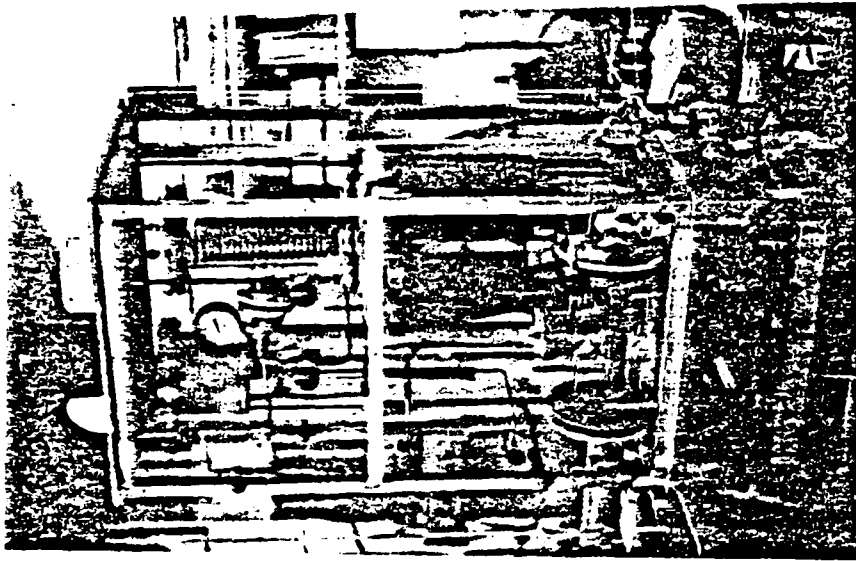


Figure 3.1. Schematic of Experimental Apparatus.



(a)



(b)

Figure 3.2. Photographs of Experimental Apparatus: (a) Water Inlet Side, and (b) Front View.

with heaters (7 and 8), and returning to the storage tank through valve (V-20). The by-pass flow path was the same up to the three-way valve then the path was through heater chamber (8) and back to the storage tank through valve (V-20). Valves V-17 and V-21 were closed in order to isolate the boiling tube. This by-pass option was essential for preheating the water to higher temperatures, to achieve higher heat flux values in the boiling tube compared to values obtained from room-temperature water. A 500-W and two 1000-W heaters were used to maintain a steady water inlet temperature and to preheat the water. Flexible pressure hose was used for water piping throughout the apparatus. The mixing chambers and sections of hose connecting the mixing chambers to the boiling tube were double insulated to ensure accurate temperature measurements.

Copper-constantan thermocouples were used to measure thermal emf's for R-114 liquid and vapor, water inlet and outlet, and water-ethylene glycol mixture. A series-connected thermopile consisting of 10 junctions on either end was used to measure the temperature drop of the water from the inlet to the outlet of the boiling tube. This thermopile was calibrated against two quartz thermometer probes and agreement was found to be better than ± 0.02 K.

B. BOILING TUBE CONSTRUCTION

Figure 3.3 shows schematics of the smooth tube, and two enhanced tubes used. The tubes tested were:

1. a smooth copper tube;
2. a 90:10 copper-nickel corrugated tube (commercially referred to as Korodense tube) with an external, sintered porous coating (i.e. High Flux);
3. an internally and externally enhanced tube (alloy C12200) produced by Wolverine Division of U.O.P. (commercially referred to as Turbo-B);
4. a porous-coated (High Flux) Korodense tube with the porous coating machined off;
5. a Turbo-B tube with the external enhancement machined off.

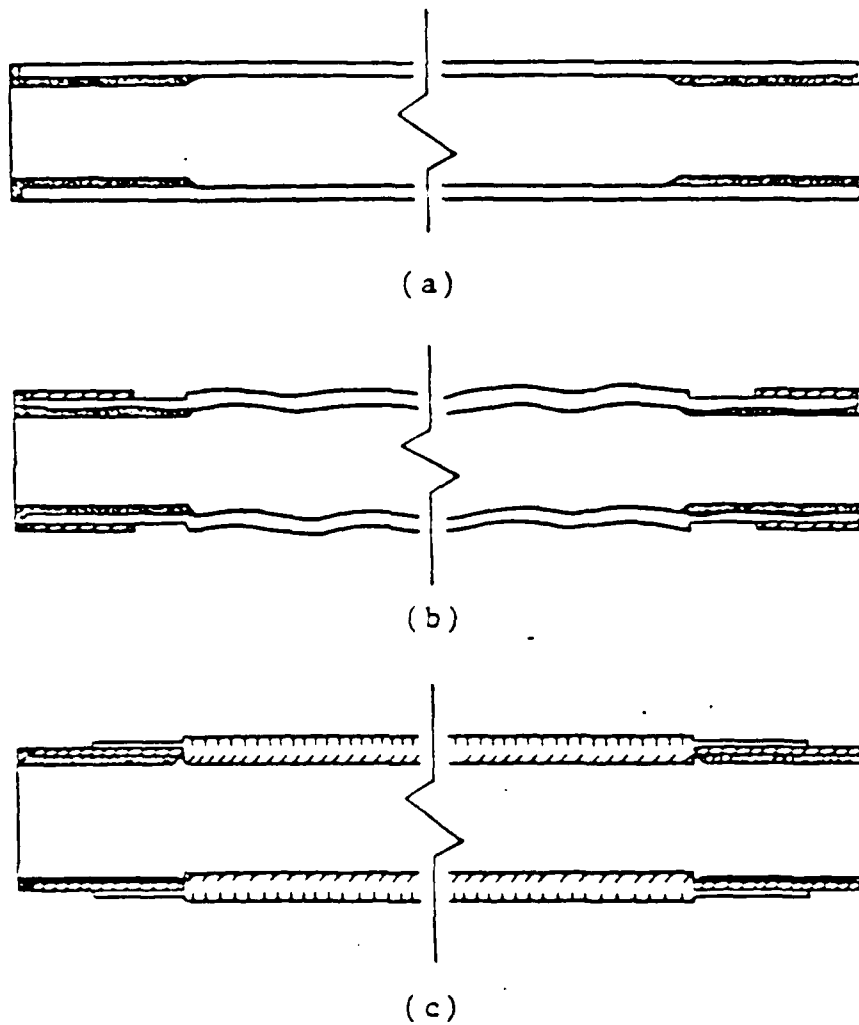
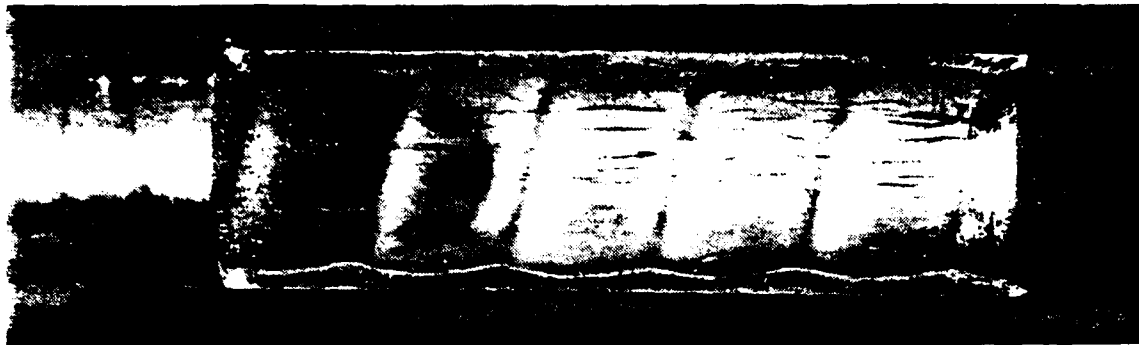
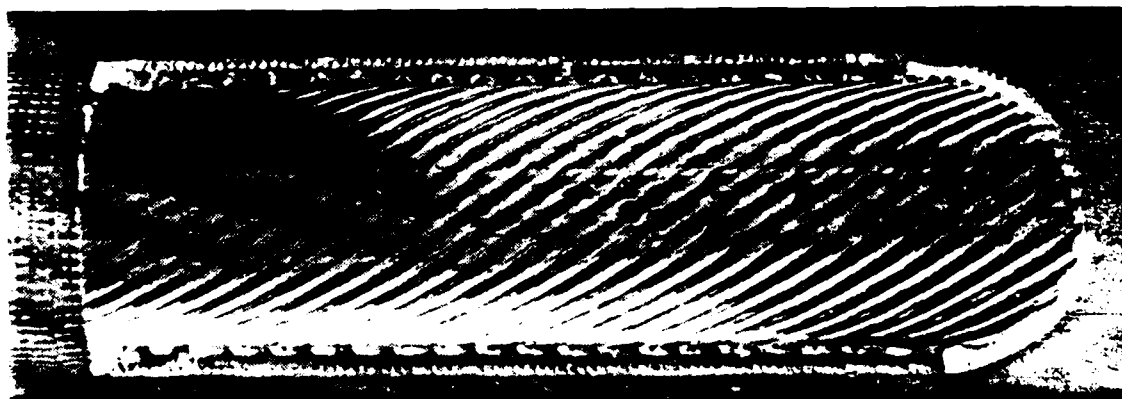


Figure 3.3. Schematic of Boiling Tubes: (a) Smooth Tube, (b) High Flux Coated Tube, and (c) Turbo-B Tube.



(a)



(b)

Figure 3.4. Photographs of Internal Enhancements:
1) Kurocense Tube, and (b) Turbo-B Tube.

These tubes will be referred to as High Flux, Turbo-B, modified High Flux, and modified Turbo-B tubes, respectively, with the exception of tubes 2 and 4. Tubes 2 and 4 will be referred to as Korodense tubes with respect to discussions of only the internal enhancement. All of the tubes had an active (i.e., heated) section of 304.8 mm in length. The smooth, High Flux, and modified High Flux tubes had an outer diameter of 15.9 mm and an inside diameter of 12.7 mm. In the case of the High Flux tube, these diameters represent the values in the smooth portion of the tube (i.e., before performing the corrugation process). The Turbo-B tube had an external structured surface and a multiple-start helical ridged inner surface. This tube had an outer diameter of 16.9 mm at the base of the external structured surface and a minimum diameter of 14.5 mm at the internal ridge tips. The modified Turbo-B tube had identical diameters as the Turbo-B tube. The 63.5-mm-long inactive sections on either end was insulated by Teflon sleeves of 1.6 mm wall thickness located inside the boiling tubes, as shown in Figure 3.3. The requirement for using these two modified tubes is explained further in Chapter IV (EXPERIMENTAL PROCEDURES).

C. COMPUTER-CONTROLLED DATA ACQUISITION AND REDUCTION

Hewlett-Packard equipment was used for data acquisition, control, and analysis, as well as for storing of data. An HP-3497A acquisition unit was used to read the thermocouple and thermopile outputs. Table 1 gives the channel designations used.

Information entered by keyboard to an HP-9826A computer unit prompted and controlled the data acquisition unit. Data were analyzed and stored with the same computer unit. A step-by-step description of the data-reduction procedure is given in Appendix A, along with a printout of the program (DRP4) used.

TABLE 1
CHANNEL DESIGNATIONS

Channel	Function
0-1	R-114 liquid thermal emf's T(1) and T(2)
2	R-114 vapor thermal emf T(3)
3	water-ethylene glycol mixture thermal emf T(4)
4	water inlet thermal emf T(5)
5	water outlet thermal emf T(6)
20	thermal emf difference across water inlet and outlet T(7)

IV. EXPERIMENTAL PROCEDURES

A. FLOWMETER CALIBRATION

This section gives a brief description of the flowmeter calibration; a more detailed explanation is given in Appendix B. A Fischer Porter flowmeter was used to indicate percent water flow through the boiling tube. Prior to conducting any boiling runs, it was necessary to develop a correlation relating the flow percent to the mass flow rate and water velocity. Additionally, any temperature effect on viscosity would be incorporated into this correlation as a correction factor. Calibration runs were conducted over a temperature range of 19 °C to 38 °C and varying flowmeter settings. The correlation (equation (B.1)) was determined from these results. The correction factor for the viscosity temperature dependency was determined to be 1.0 with an accuracy of ± 0.02 as explained in Appendix B. In fact, it was not possible to find a systematic trend for this correction factor with the water inlet temperature. The stated accuracy mainly consists of the uncertainties involved with the visual reading of the flowmeter settings.

B. BOILING TUBE AND APPARATUS PREPARATION

The external surface of the boiling tube was cleaned with a Nitrol (2% nitric acid and 98% ethyl alcohol) solution and both the external and internal surfaces were rinsed with acetone and were air dried prior to installation in the apparatus. A vacuum test at an absolute pressure of about 50 mm Hg was conducted on the refrigerant side of the apparatus after the boiling tube was installed. If no signs of leaks were evident after two hours, the system was pressurized to a gage pressure of about 250 mm Hg with R-114 vapor and the apparatus was checked for leaks with an automatic Halogen

Leak Detector. After fixing any leaks that may have been present, R-114 liquid was transferred from the reservoir to a pre-determined level in the boiling tee. This level gave a free surface 40 mm above the centerline of the boiling tube. At the set level, the mass of the R-114 liquid was computed to be 2.48 kg. A desired saturation temperature of 4 °C and the resultant system pressure were obtained by turning on the R-12 refrigeration system and varying the flow of cold (approximately -16 °C) water-ethylene glycol mixture through the condenser coil with valve V-9. At this saturation temperature and pressure, each boiling tube developed nucleation sites. The saturation temperature of 4 °C was maintained for at least 30 minutes prior to initiating nucleate boiling on the complete active length of the boiling tube.

The initiation of nucleate boiling could be done with cold water at 19 °C or with warm water at 25 °C through valve V-17 or with steam from a steam generation system through valve V-22. Early experimental data showed slight differences (up to 10 percent) in the computed outside heat-transfer coefficient depending on the highest heat flux at which the boiling was initiated on each boiling tube. As will be discussed in Chapter V (RESULTS AND DISCUSSION), the steam initiation method provided the highest initial wall superheat and ensured the best possible repeatability of the data. This initiation method was used for all of the runs unless otherwise specified.

Steam initiation was conducted by introducing steam through valve V-22 and discharging steam drain valve V-18 for about one minute. After this period, the three-way valve V-16 was shifted from a neutral position to the normal flow position. Valves V-22 and V-18 were closed and valve V-21 was opened simultaneously as the three-way valve was shifted to the normal position. Valve V-17 was opened wide prior to

shifting of the three-way valve. As these valves were shifted, warm water at 25 °C was pumped through the boiling tube at the maximum water velocity, which in turn gave the maximum heat flux for the given water inlet temperature.

C. BOILING DATA RUNS

Once the nucleate boiling initiation was completed, the saturation temperature was raised to 13.8 °C by adjusting valve V-9. This valve was also used to maintain this saturation temperature within ± 0.05 K throughout a boiling run. The water inlet temperature was maintained to within ± 0.08 K by using the heaters or introducing filtered cold water, respectively. The combination of heaters and cold water was used to maintain the desired water inlet temperature during each run. Two types of boiling runs were conducted at each oil mass percent.

The first type of run was conducted after holding the desired saturation temperature, water inlet temperature and initial flowmeter setting at steady-state conditions for about 10 minutes. After this period, the flowmeter setting was decreased with two data sets being taken at each flow setting. The two data sets were to show repeatability at each setting. The period between pairs of data sets was about 5 to 8 minutes, with steady state for each flowmeter setting maintained for at least 2 minutes. The second type of boiling run consisted of maintaining the previously mentioned initial steady-state conditions at a selected high water inlet temperature. The run was commenced by introducing cold water into the storage tank which lowered the water inlet temperature. While holding the water velocity constant, six to seven data points were taken, on a one time pass, at about every 0.3 K inlet temperature decrease. When the inlet temperature reached a selected low temperature, the steady-state conditions of the low inlet temperature,

water velocity, and saturation temperature of 13.8 °C were maintained for about 10 minutes. Then, the water inlet temperature was increased using the heaters, while holding the water velocity constant. Again, data points were taken on a one time pass, in about 0.3 K intervals, until the inlet temperature reached the previously used high inlet temperature.

Two complete boiling runs of the first type mentioned above were performed at 0% and 2% oil concentrations to further demonstrate repeatability. Table 2 shows the percent difference in wall superheat (i.e., ΔT) and heat flux for each boiling tube at these two oil percents. The higher percentages for the High Flux and Turbo-B tubes for the wall superheats are simply because of the low wall superheat values of these two tubes when compared to the values for the smooth tube. At these low superheat values, a small difference in the wall superheat leads to a larger percentage difference than that which occurs at higher wall superheats. The variation of the water inlet temperature was not considered a factor in this percent difference as the variation was less than ± 0.02 K per minute during these constant-inlet-temperature, decreasing-water-velocity runs.

TABLE 2
BOILING RUN REPEATABILITY

Tube	Oil%	ΔT	q
Smooth	0	$\pm 9\%$	$\pm 20\%$
High Flux	0	$\pm 30\%$	$\pm 12\%$
Turbo-B	0	$\pm 30\%$	$\pm 4\%$
Smooth	2	$\pm 10\%$	$\pm 25\%$
High Flux	2	$\pm 10\%$	$\pm 2\%$
Turbo-B	2	$\pm 30\%$	$\pm 2\%$

Note: initiations performed with steam

Additionally, data runs were conducted to determine the temperature increase across the boiling tube due to the pressure drop between the locations of the thermopile

probes. The data collected showed that this difference was less than the ± 0.02 K accuracy of the thermopile and was considered negligible.

Following the boiling runs in pure R-114, oil was introduced to the boiling tee through valve V-1 from the graduated cylinder (5) shown in Figure 3.1. After the required volume of oil for a given oil mass percent was added, water at the maximum velocity was pumped through the boiling tube to promote vigorous boiling. This boiling ensured good mixing of the R-114 and oil mixture. Either another boiling run was conducted or the system was shut down to prepare for another steam initiation.

D. DATA ACQUISITION AND REDUCTION

The automatic data acquisition system was prompted to record the required thermal emf's, by keyboard inputs to the computer. The data were immediately processed and printed out on a hard-copy printer. A step-by-step procedure of data processing and reprocessing is given in Appendix A. Also, a printout of the data reduction program, DRP4, is included in this appendix. The heat flux, overall heat-transfer coefficient, outside boiling heat-transfer coefficient, and wall superheat values were computed based on the outside area expressed by the diameter if the enhancement of the outer surface was removed. Further, in order to account for the heat conduction through the inactive end sections, a correction was made for heat flux using an iterative computation procedure based on natural convection as discussed by Karasbun [Ref. 20: pp. 54-56].

When a boiling run was completed, the data were reprocessed by computer to obtain the inside and outside heat-transfer coefficients for further calculations. A Sieder-Tate-type constant (C_i) for the inside coefficient for each of the externally smooth tubes was calculated by using a modified Wilson plot [Ref. 22]. For the smooth tube,

modified High Flux, and modified Turbo-B tubes, the outside coefficient was calculated simultaneously using the correlation (equation: (C.3) and (C.4)) developed by Rohsenow [Ref. 23: p. 969], and the modified Wilson plot. The Rohsenow correlation is based on externally smooth tubes, thus the requirement for the modified High Flux and Turbo-B tubes. A further explanation of the modified Wilson plot is given in Appendix C. The C_i values found for the externally smooth tubes were used for the corresponding externally enhanced tubes. Knowing the inside coefficient, the outside coefficient for the boiling tubes were computed by subtracting the inside and wall resistances from the measured overall thermal resistance (equation: (C.7)).

V. RESULTS AND DISCUSSION

A. INSIDE HEAT-TRANSFER COEFFICIENT

Results were obtained for the smooth, High Flux, and Turbo-B boiling tubes at a boiling temperature of 13.8°C and at oil concentrations of 0, 1, 2, and 6 mass percent. The heat flux versus wall superheat for these three tubes is shown in Figure 5.1. All three tubes are in the nucleate boiling range with decreasing heat flux. It can be seen that the High Flux and Turbo-B tubes outperform the smooth tube throughout the tested heat flux range. Additionally, the Rohsenow correlation for a smooth tube at a boiling temperature of 13.8°C with the experimentally determined (from the modified Wilson plot) C_{sf} coefficient of 0.0060 is shown in this figure.

The Rohsenow correlation, as used in the modified Wilson plot, has an exponent of $r = 1/3$. Yet, this correlation is very sensitive to the r value. A change in this exponent of three percent yielded a change in the C_{sf} only of 0.016 percent but gave a change of 17 percent in the Sieder-Tate-type constant inferred from the modified Wilson plot. For the purpose of data analysis, the value of $r = 1/3$ was used, while knowing that an additional uncertainty was being introduced by this exponent.

For each externally smooth tube, the Sieder-Tate-type constant was computed using the modified Wilson plot based on 5 to 10 different runs in pure R-114. The computed values for the smooth, Korodense, and Turbo-B tubes were 0.021 ± 0.005 , 0.066 ± 0.005 , and 0.077 ± 0.003 , respectively. For the smooth tube, the experimentally found Sieder-Tate-type constant is 33 percent greater than the well known value of 0.027 for long internally smooth tubes with fully developed flow. This larger constant

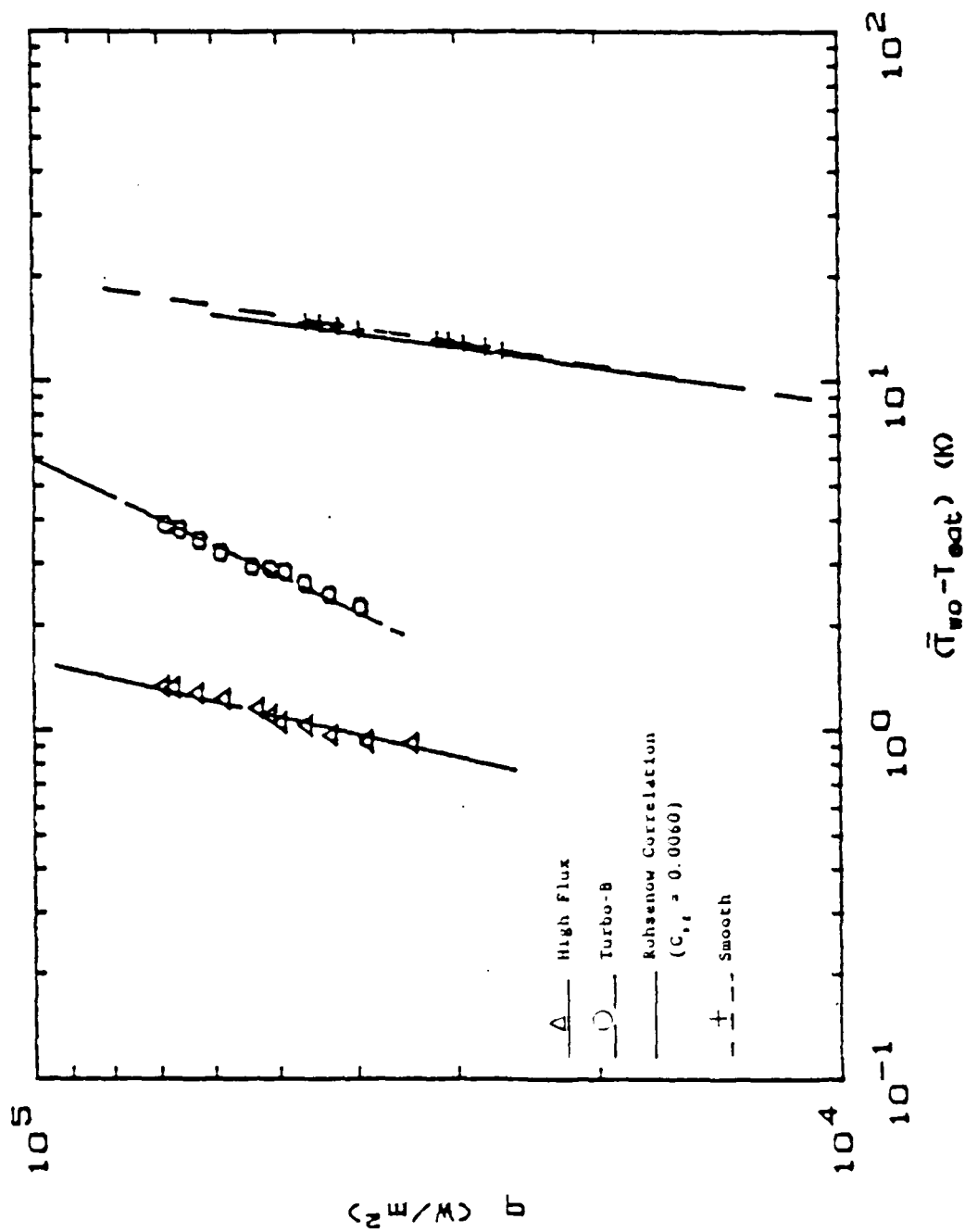


Figure 5.1. Variation of Heat Flux with Wall Superheat at 0% Oil.

appears to be the result of the entrance effects of the shorter experimental tube and the uncertainty introduced by the exponent r of the Rohsenow correlation as discussed above. The minimum entrance length for a fully developed pipe flow is given, as a rule of thumb, by Incropera and DeWitt [Ref. 24: p. 406] as

$$\frac{L_e}{D} = 60 \quad (5.1)$$

for Reynolds numbers greater than or equal to 10000. Also, as the pipe roughness increases the minimum entrance length decreases.

Withers has developed Stanton number correlations for tubes with single-helix and multiple helix ridging [Refs. 25,26: pp. 52-56,44]. These correlations are listed below. For single-helix ridging,

$$St = \frac{\sqrt{\frac{f}{3}} Pr^{-0.5} \left(\frac{p}{d}\right)^{0.33}}{7.22 \left[\left(\frac{e}{d_i}\right) Re \left(\frac{f}{3}\right)^{0.5} \right]^{0.127} + \gamma} \quad (5.2)$$

$$\sqrt{\frac{f}{3}} = - \frac{1}{2.46 \ln \left[r + \left(\frac{e}{Re}\right)^m \right]} \quad (5.3)$$

where r and m are determined by tube dimensions, and

$$\gamma = - \left\{ 2.51 \ln \left[2 \left(\frac{e}{d_i}\right) + 3.75 \right] \right\} \quad (5.4)$$

For multiple-helix ridging,

$$St = \sqrt{\frac{f}{3}} Pr^{-0.5} \left[\frac{1}{3^{\frac{1}{4}} \left(Re \sqrt{\frac{f}{3}} \right)^{0.136} + \gamma} \right] \quad (5.5)$$

$$\sqrt{\frac{f}{3}} = - \frac{1}{2.46 \ln \left[r + \left(\frac{e}{Re}\right)^m \right]} \quad (5.6)$$

r and m again are functions of tube dimensions,

$$\gamma = - \left\{ 2.5 \ln \left[2 \left(\frac{e}{D_i} \right) + 3.75 \right] \right\} \quad (5.7)$$

and

$$S^* = 5.63 \left(\frac{e}{D_i} \right)^{-\frac{1}{3}} \left(\frac{e}{D_i} \right)^{0.136} \quad (5.8)$$

A comparison of Stanton numbers was made for the modified Korodense and modified Turbo-B tubes using the following equations for these two tubes:

$$St = \frac{h_i D_i}{k_f Re Pr} \quad (5.9)$$

where

$$h_i = C_i \frac{k}{D_i} Re^{0.3} Pr^{0.33} \left(\frac{u}{u_w} \right)^{0.14} \quad (5.10)$$

The results for these two modified tubes were compared to a copper Korodense (i.e., single-helix ridging) and a Turbo-Chill (i.e., multiple-helix ridging) tubes, respectively. The latter two tubes tested by Withers were similar in radial dimensions but were 1.5 meter long. The predicted St numbers using equations (5.1) - (5.8) for the Withers' Korodense and Turbo-Chill tubes were 0.00177 and 0.00273, respectively. The experimental St numbers using equations (5.9) and (5.10) for the modified Korodense and modified Turbo-B tubes were 0.00242 and 0.00286, respectively. The majority of the difference between the predicted and experimental St numbers may be attributable to the entrance effects and the uncertainty introduced by the Rohsenow correlation.

B. LIGHT OFF EFFECTS

As referred to in Chapter IV, Figure 5.2 shows the light off effects for the smooth, High Flux (i.e., porous-coated Korodense), and Turbo-B tubes. These effects are most probably due to the requirement of greater heat flux to initiate

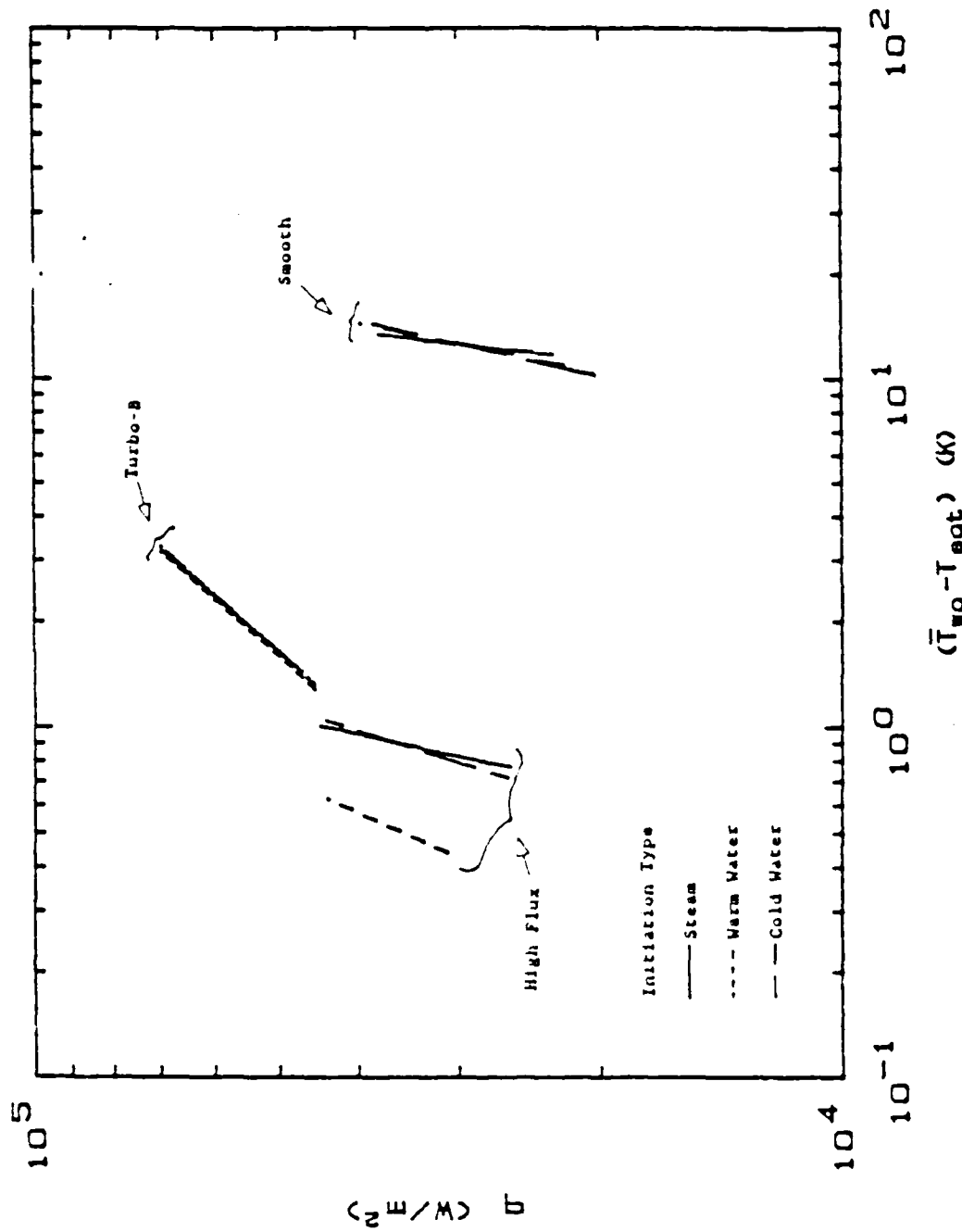


Figure 5.2. Light Off Effects at 0% Oil.

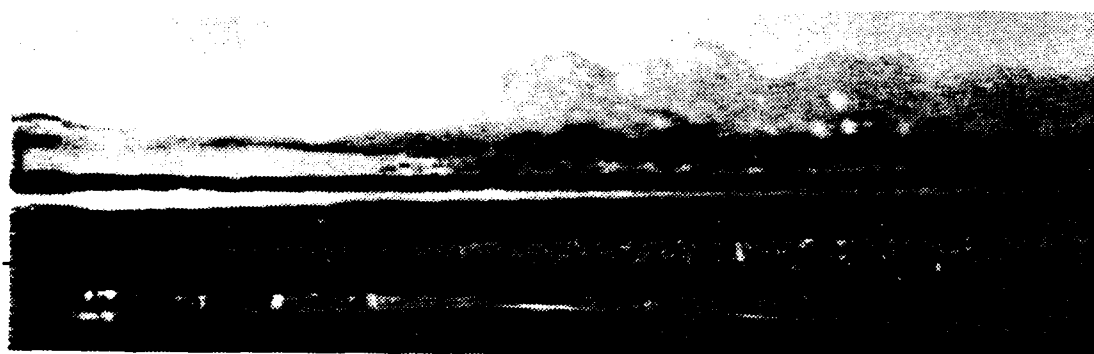
the nucleation sites than the heat flux required to maintain the sites once they are activated. As the boiling tube sits in the R-114 liquid, prior to initiation, reentrant cavities or the nucleation sites flood with liquid. The initial formation of the vapor bubbles and thus the initiation of the nucleation site requires the input of a greater heat flux or higher wall superheat. Figure 5.3 shows the boiling tube initiation with steam for the smooth, High Flux, and Turbo-B tubes [Refs. 21,7: p. 478, 62]. As shown in Figure 5.3, the High Flux tube is more sensitive to light off effects. This sensitivity is mostly due to the lower wall superheats at which nucleation occurs. A change of .5 of a degree is more pronounced at these lower wall superheats than a similar change at the wall superheats for the Turbo-B and smooth tubes.

C. SMOOTH TUBE

Figure 5.4 shows the performance of the smooth tube at 0, 1, 2, and 6 mass percent oil concentration at 13.8 °C. Reilly's [Ref. 8: p. 65] data for the electrically heated smooth tube at a boiling temperature of -2.2 °C in pure R-114 liquid are also included for comparison. The differences between the experimental results shown and Reilly's data are probably due to physical characteristics introduced in the electrically heated tube when soldering the copper sleeves (inside of which the electric heaters were fitted) on the interior of the tube. As discussed by Reilly [Ref. 8: pp. 57-61], the contact resistance at the interface between the sleeve and the inner surface of the tube was minimized by tinning. However, the tinning process may not have been 100 percent successful, thereby introducing unacceptable uncertainties into the experimental measurements. Further Reilly reported considerable variations (up to 3 K at a heat flux of 98 kW/m²) in the measured wall temperatures. Reilly attributed this observation to an axially non-uniform heat flux generated by the cartridge heater.



(a)



(b)



(c)

Figure 5.3. Photographs of Steam Initiation: (a) Smooth Tube
(b) High Flux Tube, and (c) Turbo-3 Tube.
Note: Bar in front of boiling tubes is an
auxiliary heater.

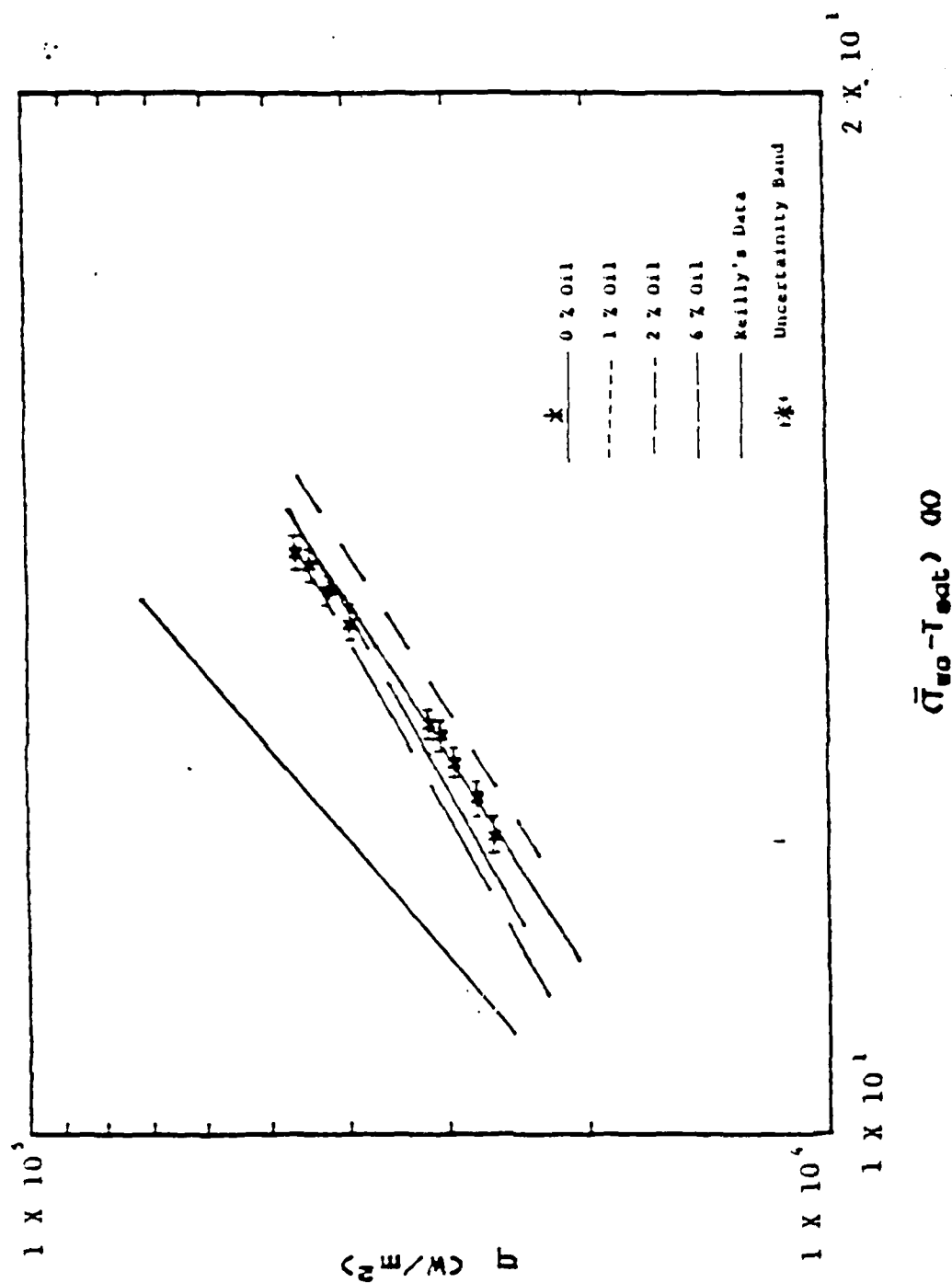


Figure 5.4. Variation of Heat Flux with Wall Superheat for Smooth Tube.

As shown in Figure 5.4, the wall superheat increased for 1 percent oil concentration and decreased slightly for 2 and 6 percent oil. This decrease in the wall superheat for the higher oil percentage is possibly due to the enhanced bubble formation experienced by the tube because of the foaming action of the R-114 and oil mixture decreasing resistance to heat transfer as explained by Chongrungreong [Ref. 5: p. 701], Nobukatsu [Ref. 27: p. 60], and Chaddock [Ref. 21: p. 474].

D. HIGH FLUX TUBE

The performance of the High Flux tube in terms of heat flux versus wall superheat is given in Figure 5.5. Additionally, this figure shows Reilly's data [Ref. 8: p. 70], for the electrically heated High Flux tube in pure R-114 at a 6.7°C boiling temperature. The presence of oil increased the wall superheat, at a heat flux of 40 kW/m^2 , by a factor of 1.22 for 1 percent oil and a factor of 2.12 for 6 percent oil. The number of nucleation sites reduced considerably and the foaming action increased significantly as the oil mass percent increased. These actions are shown in Figure 5.6. With 6 percent oil concentration, it was visually observed that the nucleation sites were active only in the corrugations, as shown in Figure 5.6 (c). This congregation of sites is due, in part, to the sparser porous coating on the high points of the tube and the decreased wall thickness in the corrugations. As a result of the corrugation process during tube manufacture, the wall thickness at the corrugation is smaller than the rest of the tube, which implies lower wall resistance. During the sintering process, the coating appears to have concentrated in these corrugations giving a thicker coating of copper particles and increased number of nucleation sites compared to the rest of the tube surface.

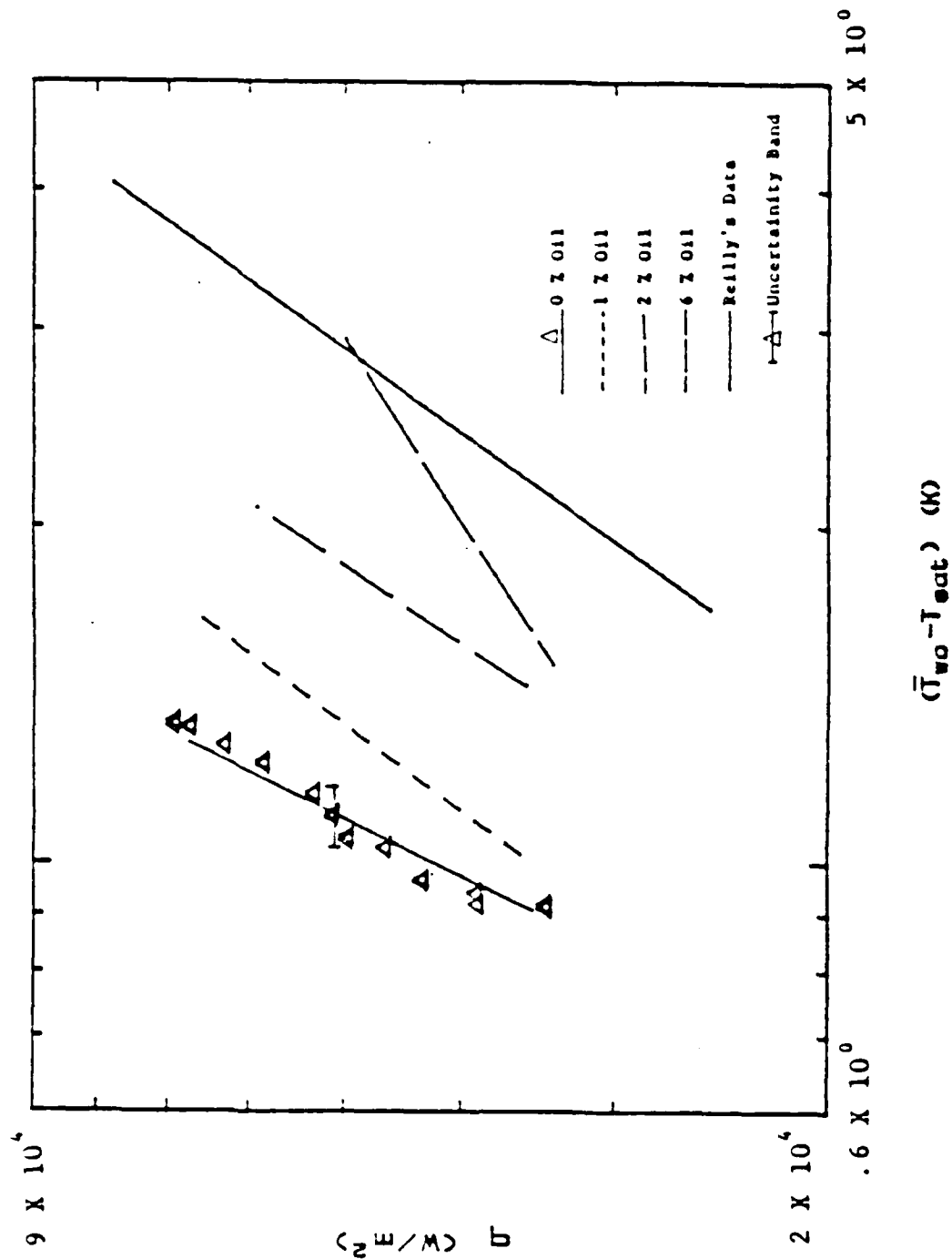
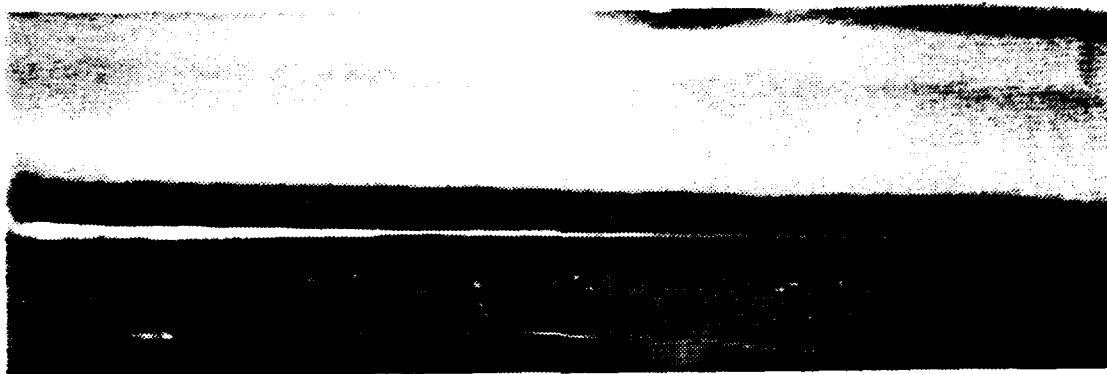


Figure 5.5. Variation of Heat Flux with Wall Superheat for High Flux Coated Tube.



(a)



(b)



(c)

Figure S.6. Photographs of Boiling from High Flux.
 Coated Tube: (a) 0%, (b) 50%, and (c) 60%.
 Note: Bar in front of boiling tube is an
 auxiliary heater

The increase of the wall superheat, when oil is present, is possibly the result of increased surface tension and viscosity. The increasing surface tension and viscosity lead to the formation of an oil-rich layer next to the boiling surface. This oil-rich layer has an insulating and inhibiting of bubble growth effect within the cavities. The higher liquid-vapor surface tension and surface tension in the oil-rich layer requires more energy for the formation and growth of the bubble. Additionally, diffusion processes affect the bubble formation. Oil concentrations near the boiling surface are high compared to the concentration in the bulk liquid and diffusion occurs from the cavity into the bulk liquid. This diffusion continues until an equilibrium point is reached. If oil-rich layers are developing on the boiling surfaces, the diffusion from the cavities to the bulk liquid slows down aiding the further build-up of the oil-rich layer. The vapor bubble forming in the cavity also has an oil vapor content which is undergoing its own diffusion process. As the refrigerant evaporates through the oil-rich layer into the interior of the bubble, it must overcome large diffusion resistances set up by the oil vapor within the bubble. The increased surface tension, viscosity, diffusion resistance and the decreasing bubble formation rate contribute to the decrease in the heat-transfer coefficient and the increase in the wall superheat at a given heat flux. [Refs. 5,21,28,29,30: p. 702, 477-478,59,372,82]

Also, boiling runs were conducted holding the water velocity constant and allowing the water inlet temperature to decrease and then to increase. The decreasing and increasing heat flux with the respective change in the water inlet temperature versus wall superheat is shown in Figure 5.7. The motion of the hysteresis (i.e., clockwise or counter-clockwise) depended on the temperature starting point. If the temperature was decreased and then increased, the motion

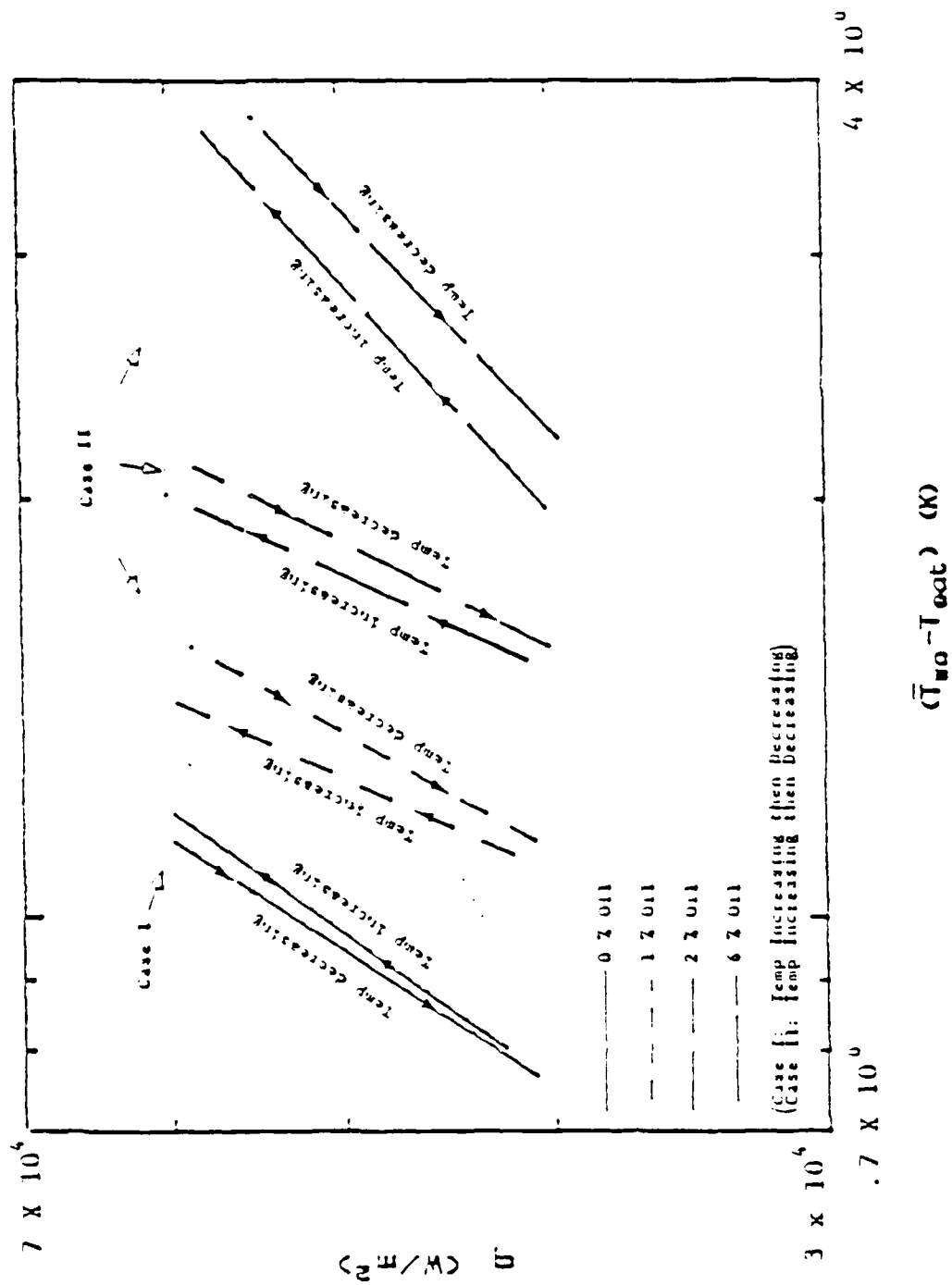


Figure 5.7. Variation of Heat Flux with Changing Water Inlet Temperature for High Flux Coated Tube.

was clockwise. When the temperature was increased and then decreased, the motion was counterclockwise. This directional change is related to the amount of heat flux required to maintain active nucleation sites. In the first case of temperature decreasing then increasing, less heat flux is needed to maintain the same amount of sites, but, at the same time, heat flux decrease as the water heat capacity is decreasing. In the second case, with the water inlet temperature increasing then decreasing, the water heat capacity increases so the heat flux increases raising the wall superheat and the heat-transfer coefficient.

E. TURBO-B TUBE

Figure 5.8 shows a similar relationship as Figure 5.5 but for the Turbo-B tube. The increase in wall superheat, for a heat flux of 40 kW/m^2 , ranges from a factor of 1.04 for 1 percent oil to a factor of 1.37 for 6 percent oil. The Turbo-B tube remained active over the full active length of the tube, as shown in Figure 5.9. The apparent decrease of nucleation sites, as shown by the High Flux tube, did not occur with the Turbo-B tube. As discussed pertaining to the High Flux tube, the increase in the wall superheat with increasing oil concentration is probably due to the increased surface tension and viscosity of the mixture within the cavities. Also, Boiling runs for constant water velocity and varying water temperature were performed on the Turbo-B tube and are also shown in Figure 5.10. The same hysteresis motions observed with the High Flux tube are observed with the Turbo-B tube.

F. COMPARISON OF BOILING HEAT-TRANSFER COEFFICIENTS

The ratios shown in Figure 5.11 are h/h_s for the Turbo-B and High Flux tubes and h/h_s for the smooth tube. All of the ratios were taken at a heat flux of 40 kW/m^2 . The High Flux tube shows the most significant effect due to oil

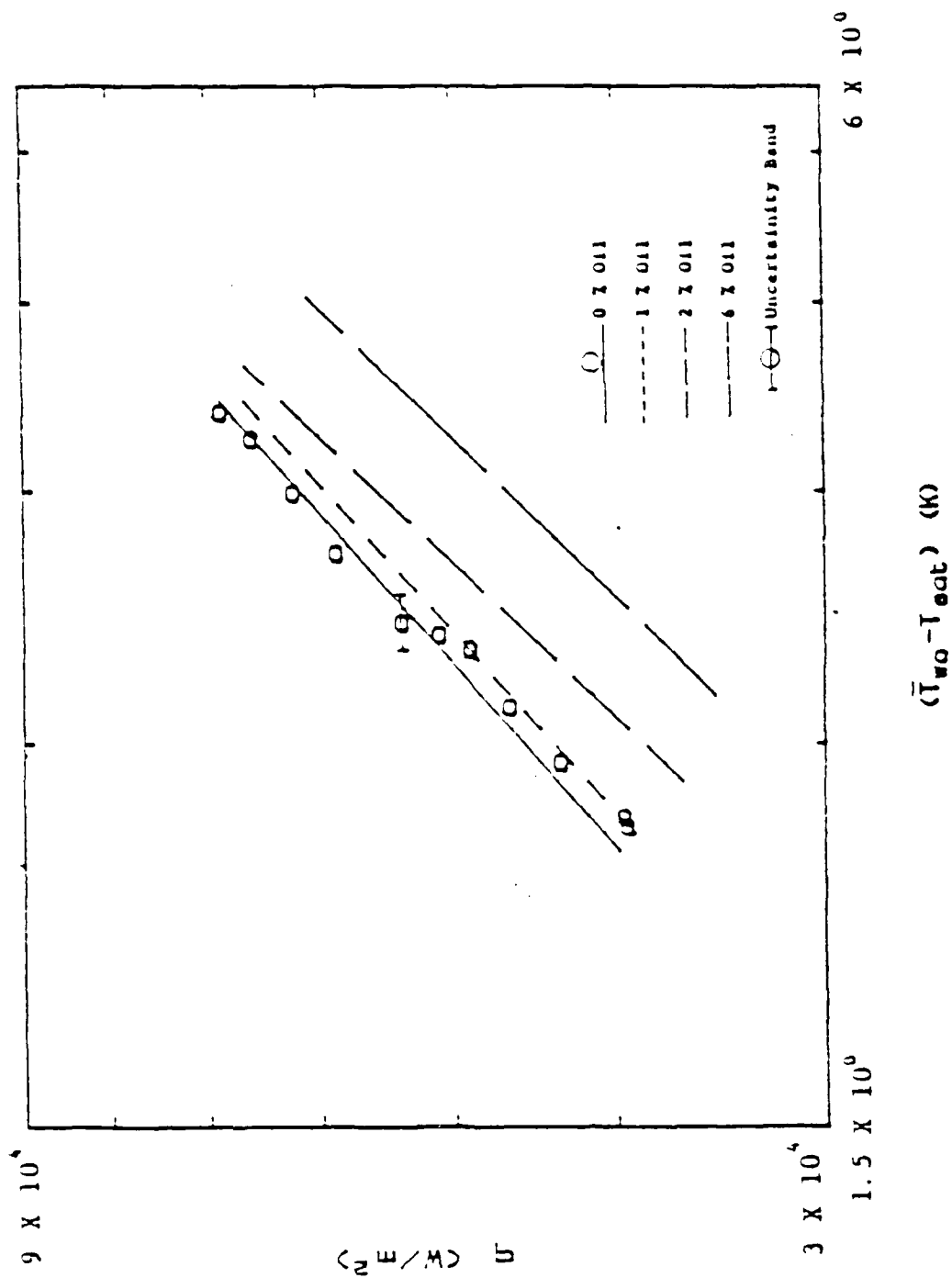
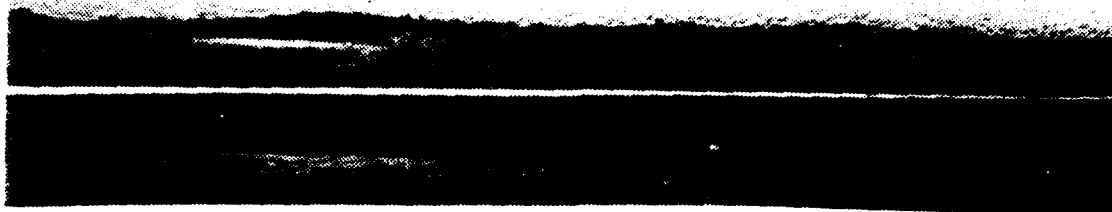
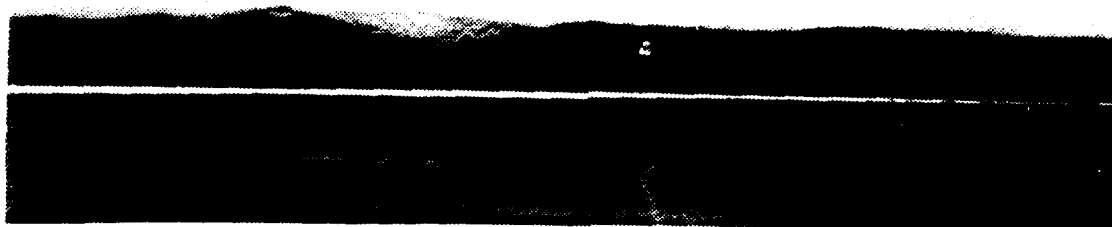


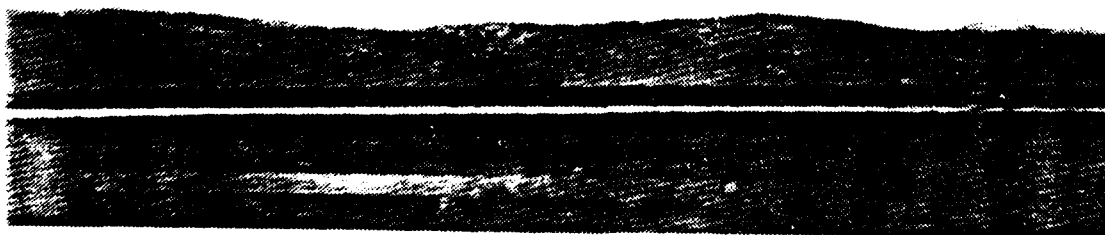
Figure 5.8. Variation of Heat Flux with Wall Superheat for Turbo-B Tube.



(a)



(b)



(c)

Figure 5.9. Photographs of Boiling from Turbo-3
Surface: (a) 0%, (b) 2%, and (c) 6%
Oil Mass Percent.
Note: Bar in front of boiling tube is an
auxiliary heater.

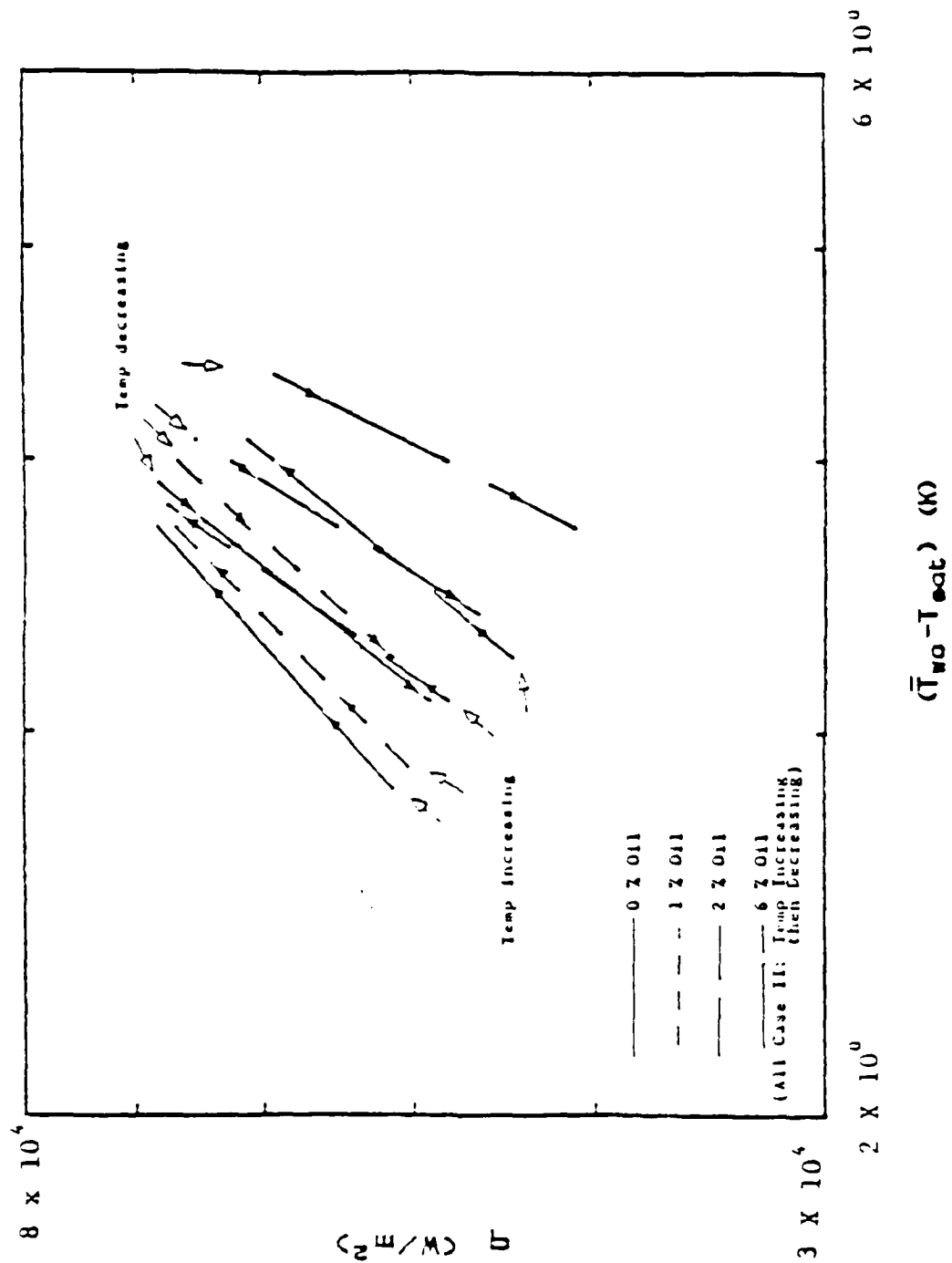


Figure 5.10. Variation of Heat Flux with Changing Water Inlet Temperature for Turbo-B Tube.

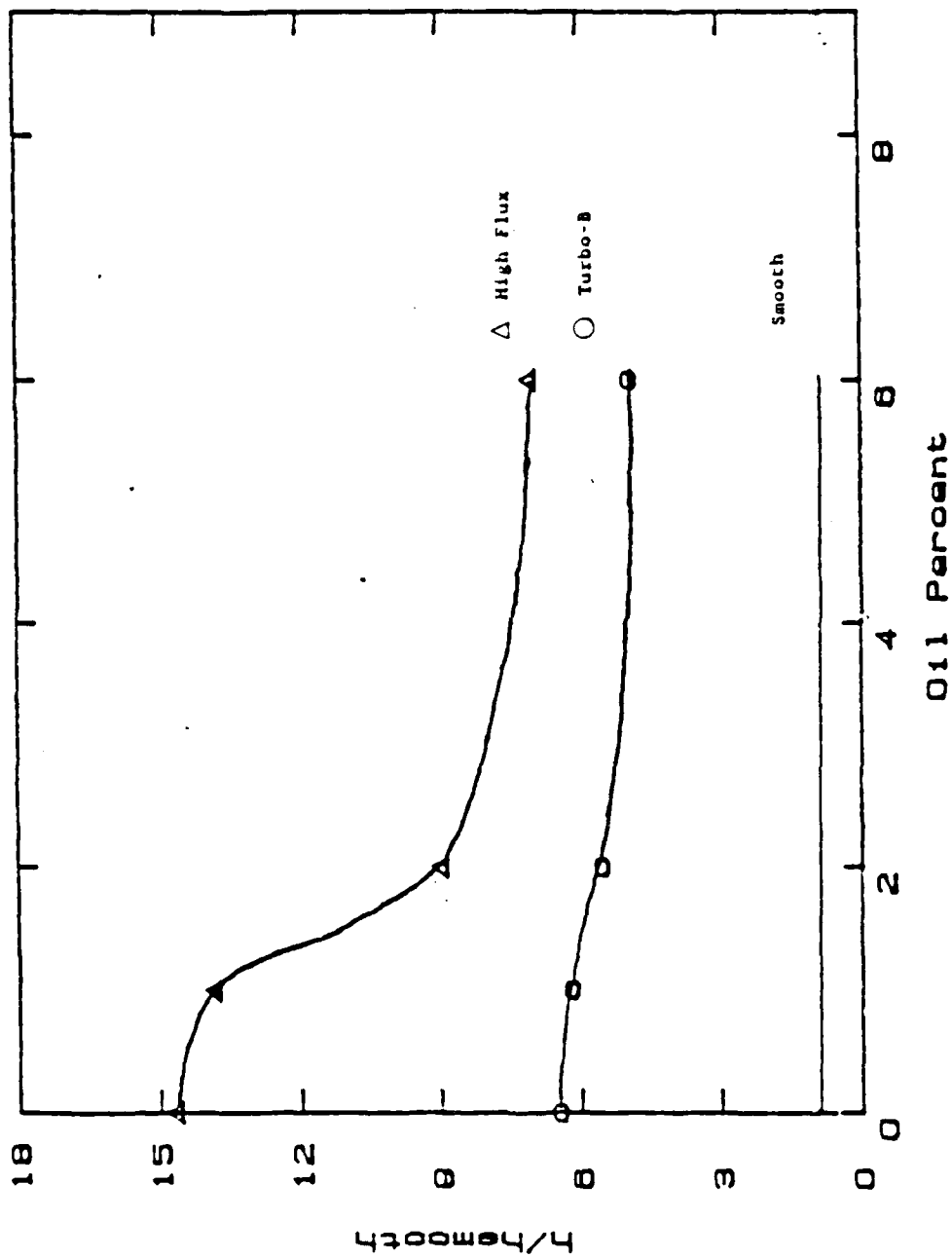


Figure 5.11. Variation of Boiling Heat-Transfer Ratio with Oil Mass Percent for a Heat Flux of 40 kW/m^2 .

concentration which is due to the reasons previously discussed. The h/h_s ratio for the High Flux tube decreased by 65 percent. For the Turbo-B tube the rate of degradation of the boiling heat-transfer coefficient is less pronounced. The Turbo-B tube shows a decrease of 24 percent at 6 mass percent oil. The larger cavity size of the Turbo-B tube, compared to the High Flux tube, results in smaller oil concentrations in the oil rich layer. This observation may explain the smaller degradation experienced by Turbo-B tube.

G. OVERALL HEAT-TRANSFER CHARACTERISTICS

The overall heat-transfer coefficient versus decreasing water velocity for oil mass percents of 0, 2, and 6 for each boiling tube is shown in Figure 5.12. For pure R-114 with a water velocity of 2 m/s, the Turbo-B tube outperforms the High Flux tube by a factor of 1.13 and the smooth tube by a factor of 4. While the High Flux tube outperformed the Turbo-B tube based on the outside heat-transfer coefficient, the reverse is true for the overall heat-transfer coefficient. This relationship in U_o is due in part to the increased internal enhancement of the Turbo-B tube. Comparison of the Sieder-Tate-type constants for the Turbo-B and High Flux tubes (see p. 34) shows that the Turbo-B tube has a 17 percent greater inside coefficient than the High Flux tube. Both of the enhanced tubes dramatically outperformed the smooth tube. It should be noted that the increase in pressure drop due to internal enhancement (compared to a smooth-interior case) was not considered here. The pressure drop would be an important factor in finally selecting the most economical tube type.

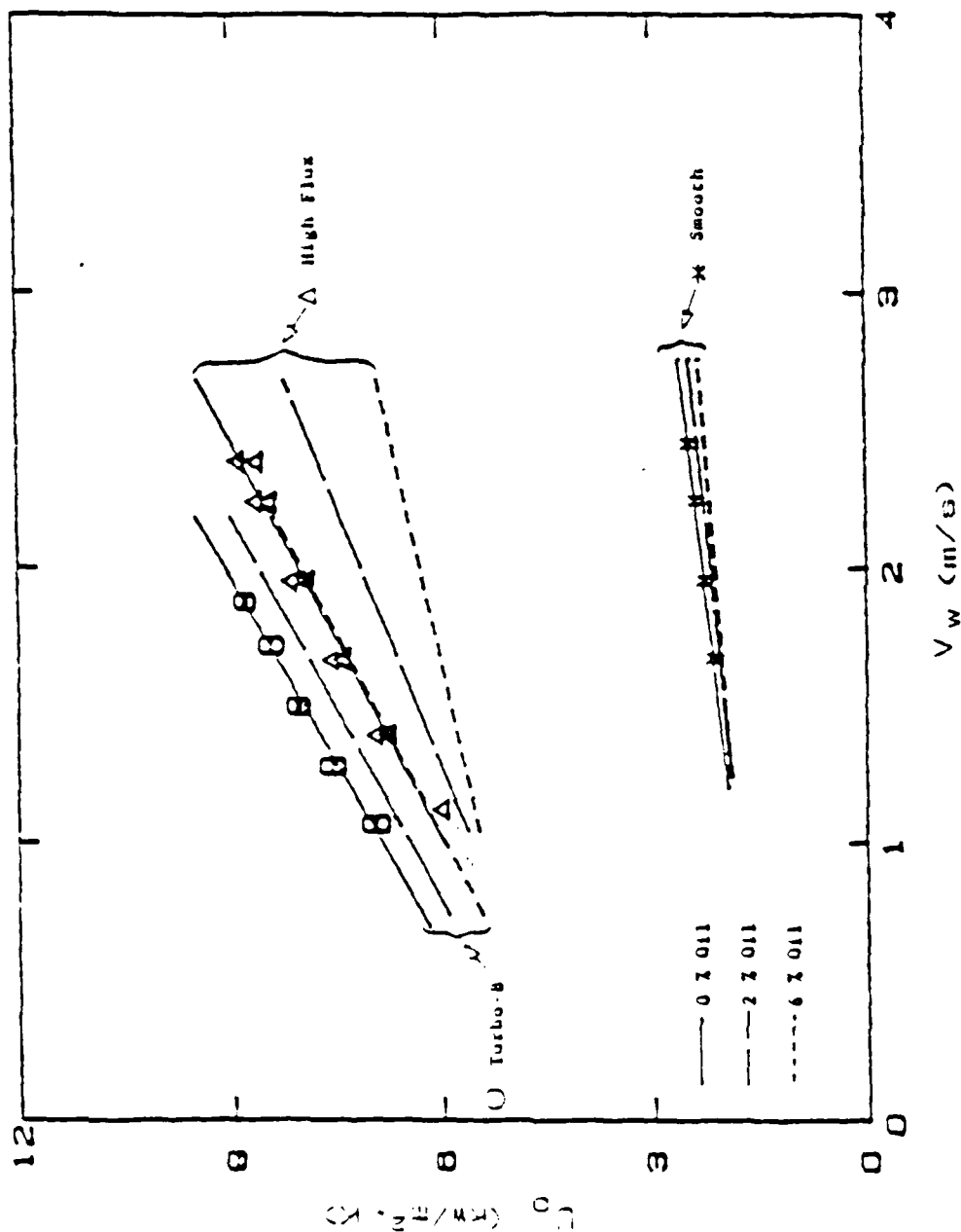


Figure 5.12. Variation of Overall Heat-Transfer Coefficient with Oil Mass Percent.

VI. CONCLUSIONS AND RECOMMENDATIONS

A. CONCLUSIONS

Considering the data gathered in this investigation for boiling of R-114 and oil mixtures at 13.8 °C boiling temperature, the following conclusions are reached:

1. Based on the overall heat-transfer coefficient, the Turbo-B and High Flux tubes outperformed the smooth tube by a factor greater than 3, and the Turbo-B tube outperformed the High Flux tube by a factor of 1.13.
2. At a heat flux of 40 kW/m² with zero mass percent oil, the outside coefficients of the High Flux and Turbo-B tubes were factors of 14.6 and 6.4 times, respectively, compared to the smooth tube. These factors decreased to 7.0 and 4.9 for the High Flux and Turbo-B tubes, respectively, with 6 mass percent oil.
3. The Turbo-B and High Flux tubes showed Sieder-Tate-type constants of 0.077 and 0.066, respectively, compared to the Sieder-Tate constant of 0.027 for long smooth tubes. As noted in the discussion, these values may be up to 10 percent lower for internally enhanced long tubes than the values for the short tubes.
4. While the High Flux tube outperformed the Turbo-B tube, based on the outside heat-transfer coefficient, the High Flux tube is more susceptible to the presence of oil.

B. RECOMMENDATIONS

Based on the results obtained from this investigation, the following recommendations are made:

1. The investigation of water-heated tubes should be upgraded to use long tubes. This would decrease the entrance effects that short tubes experience and it would come closer to duplicating actual operating conditions. Also, the pressure drop effect previously mentioned in Chapter V (RESULTS AND DISCUSSION) could be investigated in the analysis of the long tubes.
2. Studies of the boiling heat-transfer coefficients should be expanded to tube bundles. The interaction of tubes within the tube bundle is a major factor in the analysis of heat-transfer data. The boiling heat-transfer coefficient may be strongly influenced by any foaming action within the bundle.
3. Further investigations should be conducted on internal tube enhancements due to the major thermal resistance being the internal resistance.
4. Modifications to the condensing side of the present apparatus would allow for studies of short water-heated tubes at lower boiling temperatures. The major

modification would involve only the increase of the condenser drain piping to handle increases in the flow rate of the refrigerant liquid.

APPENDIX A
DATA REDUCTION PROGRAM

The data reduction program, DRP4, used for this investigation is listed below. A brief description of the major sections is given in Table 3, which is followed by an individual line listing of DRP4.

TABLE 3
DRP4 MAJOR SECTIONS

Line Number	Description
10-80	Selection options (i.e. process data, plot, etc.)
80-3690	Sub Program Main -boiling tube dimensions -select desired operating conditions (i.e. initiation mode, flow rate, Tsat, etc.) -convert emf's to temperatures -compute contact resistance (electrically heated mode only) -compute various water properties -various heat transfer calculations(Q, LMTD, U, etc.) -compute various Freon 114 properties -compute natural convective heat-transfer coefficient for unenhanced ends(iterative procedure) -compute heat loss for unenhanced ends -compute actual heat flux and boiling coefficient -record and store data
3700-4165	Functions for curve fits of various Freon 114 properties
4170-4220	Function for polynomial curve fit
4225-4935	Sub Program Poly -calculate nth order polynomial
4940-6175	Sub Program Plin -plot linear graphs
6180-6410	Sub Program Stats -calculate standard deviations
6415-6490	Sub Program Coeff -plot cross-plot files
6495-7280	Sub Program Wilson -calculate modified Wilson plot values (see Appx. C)
7285-7390	Functions for curve fits of various water properties
7395-9640	Sub Program Plot -plot non-linear graphs
9645-9725	Sub Program Symb -print various symbols on plotted graphs
9730-9755	Sub Program Purge -purge unwanted files
9760-10200	Sub Program Tdcn -calculate water temperature rise corrections due to pressure drop between thermopile locations
10205-10360	Sub Program U plot -print U files
10365-10475	Sub Program Select -select various sub program options

```

100  FILE NAME: DRP4
101  DATE: 10/00/86 10:10:10
102  REVISED: April 17, 1986
103
104  COM /Ipp/ Ipp
105  PRINTER IS :
106  CALL Select
107  INPUT "WANT TO SELECT ANOTHER OPTION (1=Y.)=N?" .Ise1
108  IF Ise1="1" THEN GOTO 40
109  BEEP
110  BEEP
111  PRINTER IS :
112  PRINT "DATA COLLECTION/REPROCESSING COMPLETED"
113  END
114  SUB Main
115  COM /Ipp/ Ipp
116  COM /C(7) C(7) .Ical
117  COM /W(17) D2.D1.D0.L.Lu.Kcu
118  DIM Emf(12),T(12),D1a(9),D2a(9),D1a(9),D2a(9),La(9),Lua(9),Kcua(9),Et(19),
119  Tns(4) (*S)
120  DATA 0.10086091,25727.94363,-767345.3295,78025595.31
121  DATA -9247486589.6,97688E+11,-2.66192E+13,3.94078E+14
122  READ C(*)
123  DATA "Smooth","High Flux","Thermoexel-E","Thermoexel-HE"
124  DATA Smooth,High Flux,Turbo-3,High Flux Mod,Turbo-3 Mod
125  READ Tns(*)
126  PRINTER IS 701
127  BEEP
128  IF Ipp=4 THEN PRINTER IS :
129  IF Ipp=4 THEN GOTO 1280
130  INPUT "ENTER MONTH, DATE AND TIME (MM:DD:HH:MM:SS)".Dates
131  OUTPUT 709:"TD":Dates
132  OUTPUT 709:"TD"
133  ENTER 709:Dates
134  PRINT
135  PRINT "          Month, date and time :":Dates
136  PRINT
137  PRINT USING "10X, ""NOTE: Program name : DRP4"""
138  BEEP
139  INPUT "ENTER DISK NUMBER".Dn
140  PRINT USING "16X, ""Disk number = "" .ZZ":Dn
141  BEEP
142  INPUT "ENTER INPUT MODE (0=3054A,1=FILE)".Im
143  BEEP
144  INPUT "SELECT HEATING MODE (0=ELEC, 1=WATER)".Ihm
145  BEEP
146  INPUT "ENTER THERMOCOUPLE TYPE (0=NEW,1=OLD)".Ical
147  IF Im=0 THEN
148  BEEP
149  INPUT "GIVE A NAME FOR THE RAW DATA FILE".D2_files
150  PRINT USING "16X, ""New file name: "" .14A":D2_files
151  D1_files=D2_files
152  CREATE BDAT D2_files,Size1
153  ASSIGN VALUE2 TO D2_files
154
155  DUMMY FILE UNTIL Num KNOWN
156  D1_files="DUMMY"
157  CREATE BDAT D1_files,Size1
158  ASSIGN VALUE1 TO D1_files

```

```

310 INPUT "ENTER NUMBER OF DEFECTIVE TCS (0=DEFAULT)".Idtc
315 IF Idtc=0 THEN
320 BEEP
325 INPUT "ENTER NUMBER OF DEFECTIVE TCS (0=DEFAULT)".Idtc
330 IF Idtc=0 THEN
335 Ldte1=0
340 Ldte2=0
345 PRINT USING "16X, ""No defective TCS exist""
350 END IF
355 IF Idtc=1 THEN
360 BEEP
365 INPUT "ENTER DEFECTIVE TC LOCATION".Ldte1
370 PRINT USING "16X, ""TC is defective at location ""'.D'":Ldte1
375 Ldte2=0
380 END IF
385 IF Idtc=2 THEN
390 BEEP
395 INPUT "ENTER DEFECTIVE TC LOCATIONS".Ldte1,Ldte2
400 PRINT USING "16X, ""TC are defective at locations ""'.D.4X.D'":Ldte1,Ldte2
405 END IF
410 IF Idtc>2 THEN
415 BEEP
420 PRINTER IS 1
425 BEEP
430 PRINT "INVALID ENTRY"
435 PRINTER IS 701
440 GOTO 310
445 END IF
450 END IF
455 OUTPUT #File1:Ldte1,Ldte2
460 ! Im=1 option
465 ELSE
470 BEEP
475 INPUT "GIVE THE NAME OF THE EXISTING DATA FILE".D2_files
480 PRINT USING "16X, ""Old file name: ""'.14A'":D2_files
485 ASSIGN #File2 TO D2_files
490 ENTER #File2:Nrun
495 ENTER #File2:Dold$
500 PRINT USING "16X, ""This data set taken on : ""'.14A'":Dold$
505 ENTER #File2:Ldte1,Ldte2
510 IF Ldte1>0 OR Ldte2>0 THEN
515 PRINT USING "16X, ""Thermocouples were defective at locations: ""'.2(0D.4X)'":
Ldte1,Ldte2
520 END IF
525 ENTER #File2:Itt
530 END IF
535 ! IF Im=0 AND Idm=1 THEN 1595
540 BEEP
545 INPUT "WANT TO CREATE A PLOT FILE? (0=N,1=Y)".Iplot
550 IF Iplot=1 THEN
555 BEEP
560 INPUT "GIVE NAME FOR PLOT FILE".P_files
565 CREATE BDA P_files.1
570 ASSIGN #Plot TO P_files
575 END IF
580 IF Idm=1 THEN
585 BEEP
590 INPUT "WANT TO CREATE A FILE? (0=N,1=Y)".Iin
595 IF Iin=1 THEN
600 BEEP

```

```

535 INPUT "ENTER Io FILE NAME".Ifiles
536 CREATE BDATA Ifiles
537 ASSIGN Iofile TO Ifiles
538 END IF
539 BEEP
540 INPUT "WANT TO CREATE Re FILE? (0=N,1=Y)".Ire
541 IF Ire=1 THEN
542 BEEP
543 INPUT "ENTER Re FILE NAME".Refiles
544 CREATE BDATA Refiles
545 ASSIGN Rofile TO Refiles
546 END IF
547 END IF
548 PRINTER IS :
549 IF Im=0 THEN
550 BEEP
551 PRINT USING "4X.****Select tube number****"
552 IF Ihm=0 THEN
553 PRINT USING "5X.****0 Smooth 4 inch Re****"
554 PRINT USING "5X.****1 Smooth 4 inch Cu (Press/Slide)****"
555 PRINT USING "5X.****2 Soft Solder 4 inch Cu****"
556 PRINT USING "5X.****3 Soft Solder 4 inch HIGH FLUX****"
557 PRINT USING "5X.****4 Wieland Hard 3 inch****"
558 PRINT USING "5X.****5 HIGH FLUX 3 inch****"
559 PRINT USING "5X.****6 GEWA-K 19 Fins/in****"
560 PRINT USING "5X.****7 GEWA-K 26 Fins/in****"
561 PRINT USING "5X.****8 GEWA-T 19 Fins/in****"
562 PRINT USING "5X.****9 GEWA-T 26 Fins/in****"
563 ELSE
564 PRINT USING "5X.****0 Smooth tube****"
565 PRINT USING "5X.****1 High Flux****"
566 PRINT USING "5X.****2 Turbo-B****"
567 PRINT USING "5X.****3 High Flux Mod****"
568 PRINT USING "5X.****4 Turbo-B Mod****"
569 END IF
570 INPUT Iitt
571 OUTPUT #File1:Iitt
572 END IF
573 PRINTER IS :
574 IF Iitt>0 THEN PRINT USING "15X.****Tube Number: ****.0****:Iitt
575 IF Iitt>9 THEN PRINT USING "15X.****Tube Number: ****.00****:Iitt
576 IF Ihm=1 THEN PRINT USING "15X.****Tube Type: ****.15A****:Iins(Iitt)
577 BEEP
578 INPUT "ENTER OUTPUT VERSION (0=LONG,1=SHORT,2=NONE)".Iov
579 BEEP
580 INPUT "SELECT (0=LIO,1=VAP,2=(LIO+VAP)/2)".Ilav
581
582 * DIMENSIONS FOR TESTED TUBES
583 * ELECTRIC HEATED MODE
584 D=Diameter at thermocouple positions
585 DATA .011125,.011125,.011125,.012954,.012446,.012954,.0100963
586 DATA .0100963,.011157,.01157
587 READ DATA
588 D=Diameter
589
590 * D=Diameter of test section to the base of fins
591 DATA .015825,.015875,.015875,.015824,.015875,.015824,.0127
592 DATA .0127,.0103,.0103
593 READ DATA
594
595 * D=inside diameter of unheated ends

```

```

910 DATA 0.0127,0.0127,0.0127,0.0127,0.0127,0.0125,0.0125,0.0118,0.0118
915 READ Dia(*)
920 ! Do=Outside diameter of unenhanced ends
920 DATA 0.015875,0.015875,0.015875,0.015824,0.015875,0.015824,0.01270,0.01270,0.01001,
925 ! 0.01001
930 READ Doa(*)
935 ! L=Length of enhanced surface
940 DATA 1.016,1.016,1.016,1.016,2.032,2.032,2.032,2.032,2.032,2.032
945 READ La(*)
950 ! Lu=Length of unenhanced surface at the ends
960 DATA 0.0254,0.0254,0.0254,0.0762,0.0762,0.0762,0.0762,0.0762,0.0762
965 READ Lua(*)
970 !
975 ! Kcu=Thermal Conductivity of tube
980 DATA 398.344,344.45,344.45,344.944,398.398
985 READ Kcua(*)
990 IF Ihm=1 THEN
995 !
1000! Data statements for water heating mode
1005!
1010 DATA 0.015875,0.015875,0.0169,0.0138,0.0169,0.0,0.0,0.0
1015 READ D2a(*)
1020 DATA 0.0127,0.0127,0.0145,0.0127,0.0145,0.0,0.0,0.0
1025 READ Dia(*)
1030 DATA 0.015875,0.015875,0.0169,0.015875,0.0169,0.0,0.0,0.0
1035 READ Doa(*)
1040 DATA 0.3048,0.3048,0.3048,0.3048,0.3048,0.0,0.0,0.0
1045 READ La(*)
1050 DATA 0.0254,0.0254,0.0254,0.0254,0.0254,0.0,0.0,0.0
1055 READ Lua(*)
1060 DATA 398.45,398.45,398.0,0.0,0.0,0.0
1065 READ Kcua(*)
1070 END IF
1075 D2=D2a(Itr)
1080 D1=Dia(Itr)
1085 D0=Doa(Itr)
1090 L=La(Itr)
1095 Lu=Lua(Itr)
1100 Kcu=Kcua(Itr)
1105 Xn=0.3
1110 F=0
1115 IF Itr=0 THEN CF=1.70E+9
1120 IF Itr>0 THEN CF=3.7037E+10
1125 A=PI*(D0*D1-D1*D2)/4
1130 P=PI*D0
1135 BEEP
1140 INPUT "TUBE INITIATION MODE: (1=HOT WATER,2=STEAM,3=COLD WATER)".Itrm
1145 IF Itrm=1 THEN PRINT USING "16X, ""TUBE Initiate: Hot Water""
1150 IF Itrm=2 THEN PRINT USING "16X, ""TUBE Initiate: Steam""
1155 IF Itrm=3 THEN PRINT USING "16X, ""TUBE Initiate: Cold Water""
1160 INPUT "TEMP/VEL MODE: (0=T-CONST,1=DEC,2=T-DEC,3=CONST,4=T-INC,5=T-CONST)".Itrv
1165 IF Itrv=0 THEN PRINT USING "16X, ""Temp/Vel Mode: Constant/Decreasing""
1170 IF Itrv=1 THEN PRINT USING "16X, ""Temp/Vel Mode: Decreasing/Constant""
1175 IF Itrv=2 THEN PRINT USING "16X, ""Temp/Vel Mode: Increasing/Constant""
1180 INPUT "WANT TO RUN WILSON PLOTS (Y/N)".Iwll
1185 IF Ihm=1 AND Iwll=0 THEN

```

```

1230 IF Ict=1 THEN Ict=10
1235 IF Ict=1 OR Ict=3 THEN C1=.059
1240 IF Ict=2 OR Ict=4 THEN C1=.062
1245 BEEP
1250 INPUT "ENTER C1 (DEF: .059 IF=.059, .062)";C1
1255 PRINT USING "5X.000" "C1=:";C1
1260 PRINT USING "5X.000" "Constant = " ".2.40";C1
1265 END IF
1270 IF Ihm=1 AND Im=1 AND Iur=1 THEN
1275 IF Ict=0 THEN C1=.059
1280 IF Ict=1 OR Ict=3 THEN C1=.059
1285 IF Ict=2 OR Ict=4 THEN C1=.062
1290 ASSIGN #File2 TO *
1295 CALL Wilson(C1,C1)
1300 ASSIGN #File2 TO D2_File5
1305 ENTER #File2:Nrun,OldS,Latc1,Latc2,Itr
1310 END IF
1315 Nsub=0
1320 IF Iap=4 THEN Ihm=1
1325 IF Ihm=1 THEN Nsub=3
1330 Ntc=5
1335 J=1
1340 Sx=0
1345 Sy=0
1350 Sxs=0
1355 Sxv=0
1360 Repeat: !
1365 IF Im=0 THEN
1370 Dtd=2.22
1375 Ido=2
1380 ON KEY 0,15 RECOVER 1020
1385 PRINTER IS
1390 PRINT USING "4X.000" "SELECT OPTION"
1395 PRINT USING "5X.000" "0=TAKE DATA"
1400 IF Ihm=0 THEN PRINT USING "5X.000" "1=SET HEAT FLUX"
1405 IF Ihm=1 THEN PRINT USING "5X.000" "2=SET WATER FLOW RATE"
1410 PRINT USING "5X.000" "3=SET Test"
1415 PRINT USING "4X.000" "NOTE: KEY 1 = ESCAPE"
1420 BEEP
1425 INPUT Ido
1430 IF Ido>2 THEN Ido=2
1435 IF Ido=0 THEN GOTO 1445
1440 !
1445 ! LOOP TO SET HEAT FLUX OR FLOWMETER SETTING
1450 IF Ido=1 THEN
1455 IF Im=0 THEN
1460 OUTPUT 109:"AR AF'2 AL'D VRS"
1465 BEEP
1470 INPUT "ENTER DESIRED Qdp";Qdpd
1475 PRINT USING "4X.000" "DESIRED Qdp ACTUAL Qdp"
1480 Err=1000
1485 FOR I=1 TO 5
1490 OUTPUT 109:"AS SA"
1495 Qum=0
1500 FOR J=1 TO 5
1505 ENTER 109:E
1510 Qum=Qum+E
1515 NEXT J
1520 IF I=1 THEN Qdp=Qum/5
1525 IF I=2 THEN Qdp=Qum/5

```

```

1490 NEXT I
1495 Aapp=Vol1+Amp/(P1-D2+L)
1500 IF ABS(Aapp-Dapp)>Err THEN
1505 IF Aapp>Dapp THEN
1510 BEEP 4000.12
1515 BEEP 4000.12
1520 BEEP 4000.12
1525 ELSE
1530 BEEP 250.12
1535 BEEP 250.12
1540 BEEP 250.12
1545 END IF
1550 PRINT USING "4X.MZ.3DE.2X.MZ.3DE":Dapp,Aapp
1555 WAIT 2
1560 GOTO 1445
1565 ELSE
1570 BEEP
1575 PRINT USING "4X.MZ.3DE.2X.MZ.3DE":Dapp,Aapp
1580 Err=500
1585 WAIT 2
1590 GOTO 1445
1595 END IF
1600 ELSE
1605 BEEP
1610 INPUT "ENTER FLOWMETER SETTING".Fms
1615 GOTO 1350
1620 END IF
1625 END IF
1630!
1635! LOOP TO GET Tsat
1640 IF Ido=2 THEN
1645 IF Ikdt=1 THEN 1670
1650 BEEP
1655 INPUT "ENTER DESIRED Tsat".Dtld
1660! PRINT USING "4X.":Tsdt ATsat Rate Tv Rate""
1665 Ikdt=1
1670 Dtld=0
1675 Dld2=0
1680 Nn=1
1685 Nrs=Nn MOD 15
1690 Nn=Nn+1
1695 IF Nrs=1 THEN
1700 PRINT USING "4X.":Tsdt Tld1 Tld2 Tv Tsump Tinlet Toile
Tout""
1705 END IF
1710 IF Ihm=0 THEN OUTPUT 709:"AR AF3 AL1 VRS"
1715 IF Ihm=1 THEN OUTPUT 709:"AR AF0 AL5 VRS"
1720 FOR I=1 TO 5
1725 IF Ihm=0 AND I>4 THEN 1860
1730 Sum=0
1735 OUTPUT 709:"AS SA"
1740 FOR J=1 TO 20
1745 ENTER 709:E...
1750 Sum=Sum+E...
1755 NEXT J
1760 E...=Sum/20
1765 E...=INT(SQRT(E...))
1770 IF E... THEN Tld1=Tld
1775 IF E... THEN Tld2=Tld
1780 IF E... THEN Tld=Tld

```

```

1735 IF Ihm=1 THEN Tsump=Tld
1736 IF Ihm=2 THEN Tinet=Tld
1735 IF Ihm=3 THEN Tout=Tld
1800 NEXT Kk
1805 IF Ihm=1 THEN
1810 OUTPUT 709:"AR AF20 AL20 VR5"
1815 OUTPUT 709:"AS SA"
1820 Sum=0
1825 FOR <k=1 TO 20
1830 ENTER 709:E
1835 Sum=Sum+E
1840 NEXT Kk
1845 Emf(7)=ABS(Sum/20)
1850 Toile=Emf(7)/3.96E-4
1855 END IF
1860 Atld=(Tld1+Tld2)*.5
1865 IF ABS(Atld-Dtld)>.2 THEN
1870 IF Atld>Dtld THEN
1875 BEEP 4000..2
1880 BEEP 4000..2
1885 BEEP 4000..2
1890 ELSE
1895 BEEP 250..2
1900 BEEP 250..2
1905 BEEP 250..2
1910 END IF
1915 Err1=Atld-Dld1
1920 Dld1=Atld
1925 Err2=Tv-Dld2
1930 Dld2=Tv
1935 IF Ihm=0 THEN PRINT USING "4X.5(MDD.0D.2X)":Dtld,Tld1,Tld2,Tv,Tsump
1940 IF Ihm=1 AND Iap=0 THEN PRINT USING "4X.7(MDD.0D.2X)":Dtld,Tld1,Tld2,Tv,Ts
ump,Tinet,Toile
1945 IF Ihm=1 AND Iap=4 THEN PRINT USING "4X.5(MDD.0D.2X).3(M3D.0D.2X)":Dtld,Tl
d1,Tld2,Tv,Tsump,Tin
1950 WAIT 2
1955 GOTO 1685
1960 ELSE
1965 IF ABS(Atld-Dtld)>.1 THEN
1970 IF Atld>Dtld THEN
1975 BEEP 3000..2
1980 BEEP 3000..2
1985 ELSE
1990 BEEP 300..2
1995 BEEP 300..2
2000 END IF
2005 Err1=Atld-Dld1
2010 Dld1=Atld
2015 Err2=Tv-Dld2
2020 Dld2=Tv
2025 IF Ihm=0 THEN PRINT USING "4X.5(MDD.0D.2X)":Dtld,Tld1,Tld2,Tv,Tsump
2030 IF Ihm=1 THEN PRINT USING "4X.5(MDD.0D.2X).3(M3D.0D.2X)":Dtld,Tld1,Tld2,Tv
,Tsump,Tinet,Toile.
2035 WAIT 2
2040 GOTO 1685
2045 ELSE
2050 BEEP
2055 Err1=Atld-Dld1
2060 Dld1=Atld
2065 Err2=Tv-Dld2

```



```

2070 31d2=tv
2075 IF ihm=0 THEN PRINT USING "4X.5(MDD.00.0X)":0t1d1,t1d2,tv,tsump
2080 IF ihm=1 THEN PRINT USING "4X.3(MDD.00.0X)":0t1d1,t1d2,t1d2,tv,tsump,tinlet
2085 31e=0
2090 GOTO 1685
2095 END IF
2100 END IF
2105 END IF
2110! ERROR TRAP FOR Ido OUT OF BOUNDS
2115 IF Ido>2 THEN
2120 BEEP
2125 GOTO 1250
2130 END IF
2135!
2140! TAKE DATA IF Im=0 LOOP
2145 IF Ikol=1 THEN 2165
2150 BEEP
2155 INPUT "ENTER BULK OIL Y".300
2160 Ikol=1
2165 IF ihm=0 THEN OUTPUT 709:"AR AFD AL11 VRS"
2170 IF ihm=1 THEN OUTPUT 709:"AR AFD ALS VRS"
2175 IF ihm=0 THEN Ntc=12
2180 FOR I=1 TO Ntc
2185 OUTPUT 709:"AS SA"
2190 Sum=0
2195 FOR J1=1 TO 20
2200 ENTER 709:E
2205 Sum=Sum+E
2210 IF I=(9-Nsub) OR I=(10-Nsub) THEN Et(J1-I)=E
2215 NEXT J1
2220 Kd1=0
2225 IF I=(9-Nsub) OR I=(10-Nsub) THEN
2230 Eave=Sum/20
2235 Sum=0
2240 FOR Jk=0 TO 19
2245 IF ABS(Et(Jk)-Eave)<5.0E-5 THEN
2250 Sum=Sum+Et(Jk)
2255 ELSE
2260 Kd1=Kd1+1
2265 END IF
2270 NEXT Jk
2275 IF I=(9-Nsub) OR I=(10-Nsub) THEN PRINT USING "4X.0000":Kd1
2280 IF Kd1>0 THEN
2285 BEEP
2290 BEEP
2295 PRINT USING "4X.0000":Too much scattering in data - repeat data set
2300 GOTO 1245
2305 END IF
2310 END IF
2315 Et(I)=Sum/(20-Kd1)
2320 NEXT I
2325 IF ihm=1 THEN
2330 OUTPUT 709:"AR AFD AL20 VRS"
2335 OUTPUT 709:"AS SA"
2340 Sum=0
2345 FOR Jk=1 TO 20
2350 ENTER 709:E
2355 Sum=Sum+E
2360 NEXT Jk
2365 Et(I)=ABS(Sum)/20

```

```

2370 END IF
2375 IF Ihm=0 THEN
2380 OUTPUT 709:"AR AF12 AL13 VRS"
2385 FOR I=1 TO 2
2390 OUTPUT 709:"AS SA"
2395 Sum=0
2400 FOR J=1 TO 2
2405 ENTER 709:E
2410 Sum=Sum+E
2415 NEXT J
2420 IF I=1 THEN Vr=Sum/2
2425 IF I=2 THEN Ir=Sum/2
2430 NEXT I
2435 END IF
2440 ELSE
2445 IF Ihm=0 THEN ENTER @File2:8op.Told$.Emf(*).Vr.Ir
2450 IF Ihm=1 THEN ENTER @File2:8op.Told$.Emf(*).Fms
2455 END IF
2460!
2465! CONVERT emf'S TO TEMP.VOLT.CURRENT
2470 Twa=0
2475 FOR I=1 TO Ntc
2480 IF Idtc>0 THEN
2485 IF I=Ldte1 OR I=Ldte2 THEN
2490 T(I)=-99.99
2495 GOTO 2545
2500 END IF
2505 END IF
2510 IF Itt<4 AND Ihm=0 THEN
2515 IF I>4 AND I<9 THEN
2520 T(I)=-99.99
2525 GOTO 2545
2530 END IF
2535 END IF
2540 T(I)=FNTvsv(Emf(I))
2545 NEXT I
2550 IF Itt<4 THEN
2555 FOR I=1 TO 4
2560 IF I=Ldte1 OR I=Ldte2 THEN
2565 Twa=Twa
2570 ELSE
2575 Twa=Twa+T(I)
2580 END IF
2585 NEXT I
2590 Twa=Twa/(4-Idtc)
2595 ELSE
2600 IF Ihm=1 THEN 2550
2605 FOR I=1 TO 3
2610 IF I=Ldte1 OR I=Ldte2 THEN
2615 Twa=Twa
2620 ELSE
2625 Twa=Twa+T(I)
2630 END IF
2635 NEXT I
2640 Twa=Twa/(3-Idtc)
2645 END IF
2650 Tld=T(9-Nsub)
2655 Tld2=T(10-Nsub)
2660 Tlda=(Tld+Tld2)*.5
2665 Tv=T(11-Nsub)

```

```

2670 IF I+K1 AND Ihm=0 THEN
2675 Tld2=-39.39
2680 Tv=(T(10)+T(11))/2
2685 END IF
2690 IF Ihm=0 THEN 2710
2695 Tsump=T(12-Nsub)
2700 Tinlet=T(13-Nsub)
2705 Tout=T(14-Nsub)
2710 IF Ihm=0 THEN
2715 Amp=ABS(Ir)
2720 Volt=ABS(Vr)*25
2725 Q=Volt*Amp
2730 END IF
2735 IF Itt=0 AND Ihm=0 THEN
2740 Kcu=FNKcu(Twa)
2745 ELSE
2750 Kcu=Kcu(Itt)
2755 END IF
2760!
2765! FOURIER CONDUCTION EQUATION WITH CONTACT RESISTANCE NEGLECTED
2770 IF Ihm=0 THEN Tw=Twa-Q*LOG(D2/D1)/(2*PI*Kcu*L)
2775 IF Ilov=0 THEN Tsat=Tlda
2780 IF Ilov=1 THEN Tsat=(Tlda+Tv)*.5
2785 IF Ilov=2 THEN Tsat=Tv
2790 IF Ihm=1 THEN
2795 Tavg=Tinlet
2800 Grad=37.9853+.104388*Tavg
2805 Tdrop=ABS(Emf(7))+1.E+5/(10*Grad)
2810 Tavgc=Tinlet-Tdrop*.5
2815 IF ABS(Tavg-Tavgc)>.01 THEN
2820 Tavg=(Tavg+Tavgc)*.5
2825 GOTO 2800
2830 END IF
2835!
2840! COMPUTE WATER PROPERTIES
2845 Kw=FNKw(Tavg)
2850 Muwa=FNMuw(Tavg)
2855 Cpw=FNCPw(Tavg)
2860 Pru=FNPrw(Tavg)
2865 Rhow=FNRRhow(Tavg)
2870 Twi=Tavg
2875!
2880! Compute Mdot
2885 Mdot=3.9657E-3+Fms*(3.61955E-3-Fms*(8.82006E-6-Fms*(1.23688E-7-Fms*4.31397E-10)))
2890! Mdot=Mdot*(1.0365-Tinlet*(1.96644E-3-Tinlet*5.252E-5))/1.0037
2895 Kat=0
2900 Q=Mdot*Cpw*Tdrop
2905 Lmtc=Tdrop/LOG((Tinlet-Tsat)/(Tinlet-Tdrop-Tsat))
2910 Uo=Q/(PI*Do*L*Lmtc)
2915 Ri=Do*LOG(Do/Di)/(2.*Kcu)
2920 Tw=Tsat+Fr*Lmtc
2925 Vw=Mdot/(Rhow*PI*Di*.25)
2930! IF Kat=0 THEN
2935! Kat=1
2940! Tdrop=Tdrop+.004*Vw.2
2945! GOTO 2710
2950! END IF
2955 Reu=Rhow*Vw*Di/Muwa
2960 f1=0.316/(Reu*.13)*Prw(.13)*Cpw(.13)*(Muwa/FMuw(Twi))*.14
2965 Twi=Tavg-Q/(PI*Do*L*f1)

```

```

2970 IF ABS(Tw1-Twlc)>.01 THEN
2975 Tw1=(Tw1+Twlc)*.5
2980 GOTO 2960
2985 END IF
2990 Tw1=(Tw1+Twlc)*.5
2995 Ho=1/(1/Uo-Do/(Di-Hi)-Rw)
3000 Thetap=Q/(Ho*PI*Do*L)
3005 Tw=Ts+Thetap
3010 Thetap=Tw-Ts
3015 IF Thetap<0 THEN
3020 BEEP
3025 INPUT "TWALL<TSAT (0=CONTINUE, 1=END)",Iev
3030 IF Iev=0 THEN GOTO 1325
3035 IF Iev=1 THEN 3535
3040 END IF
3045 END IF
3050!
3055! COMPUTE VARIOUS PROPERTIES
3060 Tfilm=(Tw+Ts)*.5
3065 Rho=FNrho(Tfilm)
3070 Mu=FNmu(Tfilm)
3075 K=FNk(Tfilm)
3080 Cp=FNcp(Tfilm)
3085 Beta=FNbeta(Tfilm)
3090 Hfg=FNHfg(Ts)
3095 Ni=Mu/Rho
3100 Alpha=K/(Rho*Cp)
3105 Pr=Ni/Alpha
3110 Psat=FNPsat(Ts)
3115!
3120! COMPUTE NATURAL-CONVECTIVE HEAT-TRANSFER COEFFICIENT
3125! FOR UNENHANCED END(S)
3130 Hbar=190
3135 Fe=(Hbar*P/(Kcu*A))*.5*Lu
3140 Tann=FNtanh(Fe)
3145 Theta=Thetap*Tann/Fe
3150 Xx=(9.31+Beta*Thetap*Do*.3*Tann/(Fe*Ni*Alpha))*.166667
3155 Yy=(1+(.559/Pr)*(9/16))*.8/27
3160 Hbarc=K/Do*(.5+.387*Xx/Yy).2
3165 IF ABS((Hbar-Hbarc)/Hbarc)>.001 THEN
3170 Hbar=(Hbar+Hbarc)*.5
3175 GOTO 3135
3180 END IF
3185!
3190! COMPUTE HEAT LOSS RATE THROUGH UNENHANCED END(S)
3195 Q1=(Hbar*P*Kcu*A).5*Theta*Tann
3200 Qc=Q-2*Q1
3205 As=PI*D2*L
3210!
3215! COMPUTE ACTUAL HEAT FLUX AND BOILING COEFFICIENT
3220 Qdp=Qc/As
3225 Htube=Qdp/Thetap
3230 Csf=(Cp*Thetap/Hfg)/(Qdp/(Mu*Hfg)+(.014/(9.31*Rho).5)*(1/3)+Pr*.17)
3235!
3240! RECORD TIME OF DATA TAKING
3245 IF Im=0 THEN
3250 OUTPUT "09:TIME"
3255 ENTER "09:TIME"
3260 END IF
3265!

```

```

3270* INPUT DATA TO PRINTER
3275 PRINTER TO 10
3280 IF Iov=0 THEN
3285 PRINT
3290 PRINT USING "10X,""Data Set Number = ""$.000.2X,""Bulk Oil % = ""$.00.0.5X.1
4A"$.30p.ToldS
3295 IF Ihm=0 THEN
3300 PRINT USING "10X,""TC No:      1      2      3      4      5      6      7
      8""
3305 PRINT USING "10X,""Temp : ""$.3(1X.MDD.0D)";T(1).T(2).T(3).T(4).T(5).T(6).T(
7).T(8)
3310 PRINT USING "10X,""Twa      Tltd      Tltd2      Tvapr      Psat      Tsump""
3315 PRINT USING "10X.2(MDD.0D.1X).1X.MDD.0D.1X.2(1X.MDD.0D).2X.MDD.0";Twa.Tld.
Tld2.Tv.Psat.Tsump
3320 PRINT USING "10X,""Thetab      Htube      Qdp""
3325 PRINT USING "10X.MDD.3D.1X.MZ.3DE.1X.MZ.3DE";Thetab.Htube.Qdp
3330 ELSE
3335 PRINT USING "10X,""Fms      Vw      Tsat      Tini      Tdrop      Thetab      q      Uo
      Ho""
3340* PRINT USING "10X.4(2D.0D.1X).Z.3D.1X.0D.0D.1X.3(MZ.3DE.1X)";Fms.Vw.Tsat.Ti
niet.Tdrop.Thetab.Qd
3345 END IF
3350 END IF
3355 IF Iov=1 THEN
3360 IF J=1 THEN
3365 PRINT
3370 IF Ihm=0 THEN
3375 PRINT USING "10X,"" RUN No      Oil%      Tsat      Htube      Qdp      Thetab""
3380 ELSE
3385 PRINT USING "10X,"" FMS      OIL%      TSAT      HTUBE      QDP      THETAB""
3390 END IF
3395 END IF
3400 IF Ihm=0 THEN
3405 PRINT USING "12X.3D.4X.0D.2X.MDD.0D.3(1X.MZ.3DE)";J.Bop.Tsat.Htube.Qdp.The
tab
3410 ELSE
3415 PRINT USING "12X.3D.4X.0D.2X.MDD.0D.3(1X.MZ.3DE)";Fms.Bop.Tsat.Htube.Qdp.T
hetab
3420 END IF
3425 END IF
3430 IF Im=0 THEN
3435 BEEP
3440 INPUT "OK TO STORE THIS DATA SET (Y=1,N=0)?"$.Ok
3445 END IF
3450 IF Ok=1 OR Im=1 THEN J=J+1
3455 IF Ok=1 AND Im=0 THEN
3460 IF Ihm=0 THEN OUTPUT @File1:Bop.ToldS.Emf(+).Vr.Ir
3465 IF Ihm=1 THEN OUTPUT @File1:Bop.ToldS.Emf(+).Fms
3470 END IF
3475 IF Iuf=1 THEN OUTPUT @UFile:Vu.Qd
3480 IF Ire=1 THEN OUTPUT @RFile:Fms.Rew
3485 IF (Im=1 OR Ok=1) AND Iplot=1 THEN OUTPUT @Plot:Qdp.Thetab
3490 IF Im=1 THEN
3495 BEEP
3500 INPUT "WILL THERE BE ANOTHER RUN (Y=1,N=0)?"$.Go_On
3505 Nprint=
3510 IF Go_On=0 THEN GOSUB
3515 IF Go_On<0 THEN Repeat
3520 ELSE
3525 IF Nprint=1 THEN Repeat
3530 END IF

```

```

3535 IF Ih=0 THEN
3540 BEEP
3545 PRINT USING "10X, ""NOTE: ""'.ZZ.'"" data runs were stored in file ""'.0A'":-
      files
3550 ASSIGN #File1 TO *
3555 OUTPUT #File2:Nrun-1
3560 ASSIGN #File1 TO 01:files
3565 ENTER #File1:Date5.Ldct1.Ldct2.Itt
3570 OUTPUT #File2:Date5.Ldct1.Ldct2.Itt
3575 FOR I=1 TO Nrun-1
3580 IF Ihm=0 THEN
3585 ENTER #File1:Boo.Told5.Emf(*).Vr.Ir
3590 OUTPUT #File2:Boo.Told5.Emf(*).Vr.Ir
3595 ELSE
3600 ENTER #File1:Boo.Told5.Emf(*).Fms
3605 OUTPUT #File2:Boo.Told5.Emf(*).Fms
3610 END IF
3615 NEXT I
3620 ASSIGN #File1 TO *
3625 PURGE "DUMMY"
3630 END IF
3635 BEEP
3640 PRINT
3645 IF Iplot=1 THEN PRINT USING "10X, ""NOTE: ""'.ZZ.'"" X-Y pairs were stored in
      plot data file ""'.1
3650 ASSIGN #File2 TO *
3655 ASSIGN #Plot TO *
3660 IF Iuf=1 THEN ASSIGN #Ufile TO *
3665 IF Ire=1 THEN ASSIGN #Rfile TO *
3670 CALL Stats
3675 BEEP
3680 INPUT "LIKE TO PLOT DATA (1=Y,0=N)?".Jk
3685 IF Jk=1 THEN CALL Plot
3690 SUBEND
3695!
3700! CURVE FITS OF PROPERTY FUNCTIONS
3705 DEF FNKcu(T)
3710! OFHC COPPER 250 TO 300 K
3715 Tk=T+273.15 10 TO K
3720 <=434-1.112*Tk
3725 RETURN K
3730 FNEED
3735 DEF FNMu(T)
3740! 170 TO 350 K CURVE FIT OF VISCOSITY
3745 Tk=T+273.15 10 TO K
3750 Mu=EXP(-4.4636+(1011.47/Tk))*1.0E-3
3755 RETURN Mu
3760 FNEED
3765 DEF FNCp(T)
3770! 130 TO 400 K CURVE FIT OF Cp
3775 Tk=T+273.15 10 TO K
3780 Cp=.40188+1.65007E-3*Tk+.51494E-5*Tk2-6.67853E-10*Tk3
3785 Cp=Cp*1000
3790 RETURN Cp
3795 FNEED
3800 DEF FNRho(T)
3805 Tk=T+273.15 10 TO K
3810 Rho=(1.13+Tk/750.05)*Tk TO R
3815 Rho=.1632+51.146414*(1/Tk)+16.413015*(1/Tk)2+17.476808*(1/Tk)3+1.119829*(1/Tk)4
3820 Rho=Rho/1060400
3825 RETURN Rho

```

```

3830 FNEID
3835 DEF FNPp(T)
3840 Pp=FNCp(T)+FNMu(T)/FNK(T)
3845 RETURN Pp
3850 FNEID
3855 DEF FNK(T)
3860 T<360 < WITH T IN C
3865 K=.071-.000261*T
3870 RETURN K
3875 FNEID
3880 DEF FNTann(X)
3885 P=EXP(X)
3890 Q=1/P
3895 Tann=(P-Q)/(P+Q)
3900 RETURN Tann
3905 FNEID
3910 DEF FNTvsv(V)
3915 COM /Cc/ C(7).Ical
3920 T=C(0)
3925 FOR I=1 TO 7
3930 T=T+C(I)*V*I
3935 NEXT I
3940 IF Ical=1 THEN
3945 T=T-5.7422934E-2+T*(9.0277043E-3-T*(-9.3259917E-5))
3950 ELSE
3955 T=T+8.626897E-2+T*(3.76199E-3-T*5.0689259E-5)
3960 END IF
3965 RETURN T
3970 FNEID
3975 DEF FNBeta(T)
3980 Rop=FNRho(T+.1)
3985 Rom=FNRho(T-.1)
3990 Beta=-2/(Rop+Rom)*(Rop-Rom)/.2
3995 RETURN Beta
4000 FNEID
4005 DEF FNHfg(T)
4010 Hfg=1.3741344E+5-T*(3.3094361E-2+T*1.2165143)
4015 RETURN Hfg
4020 FNEID
4025 DEF FNPsat(Tc)
4030! 0 TO 30 deg F CURVE FIT OF Psat
4035 Tf=1.3*Tc+32
4040 Pa=5.345525+Tf*(.15352082+Tf*(1.4840963E-3+Tf*9.6150671E-6))
4045 Pg=Pa*.47
4050 IF Pg>0 THEN      ! +=PSIG, -=in Hg
4055 Psat=Pg
4060 ELSE
4065 Psat=Pg*29.32/.47
4070 END IF
4075 RETURN Psat
4080 FNEID
4085 DEF FNHsmooth(X,Bop,Isat)
4090 DIM A(5),B(5),C(5),D(5)
4095 DATA .20525,.25322,.312048,.55322,.79909,.100253
4100 DATA .74515,.72292,.72129,.71225,.66472,.64197
4105 DATA .41092,.17725,.25142,.54206,.31915,.10845
4110 DATA .71400,.72913,.72565,.53663,.665867,.51389
4115 READ A(1),B(1),C(1),D(1)
4120 IF Bop<5 THEN Isop=500
4125 IF Bop=5 THEN Isop=4

```

```

4141 IF Bop=1 THEN T=500 I=5
4142 IF Bop=1 THEN T=500
4143 Hs=EXP(A(I)+B(I)+LOG(X))
4144 ELSE
4145 Hs=EXP(C(I)+D(I)+LOG(X))
4146 END IF
4147 RETURN Hs
4148 FNEND

5495 SUB Wilson(Cf,Ci)
5500 COM /W11/ 02.01.00.Lu.Kcu
5505 DIM Emf(10)
5510! ALISON PLOT SUBROUTINE DETERMINE CF AND CI
5515 BEEP
5520 INPUT "ENTER DATA FILE NAME".File5
5525 BEEP
5530 PRINTER IS 1
5535 PRINT USING "4X." "Select option:"
5540 PRINT USING "4X." " 0 Vary Cf and Ci"
5545 PRINT USING "4X." " 1 Fix Cf Vary Ci"
5550 PRINT USING "4X." " 2 Vary Cf Fix Ci"
5555 PRINT USING "4X." " 3 Fix Cf Fix Ci"
5560 INPUT "ENTER OPTION".Icfix
5565 PRINTER IS 701
5566 IF Icfix=0 THEN 5585
5570 IF Icfix>0 THEN BEEP
5575 IF Icfix=1 THEN INPUT "ENTER Cf".Csf
5580 IF Icfix=2 THEN INPUT "ENTER Ci".Ci
5581 IF Icfix=3 THEN INPUT "ENTER Cf, Ci".Csf,Ci
5585 PRINTER IS 1
5590 INPUT "Want To Vary Coeff?(1=Y,0=N)".Iccoeff
5595 IF Iccoeff=1 THEN INPUT "ENTER COEFF".R
5600 PRINTER IS 701
5605 IF Icfix=0 OR Icfix=2 THEN Cfa=.004
5610 IF Icfix=1 THEN Cfa=Csf
5615 Cia=Ci
5620 Xn=.3
5625 Fr=.3
5630 Uj=0
5635 Rr=.3
5640 IF Iccoeff=1 THEN Rr=R
5645 PRINTER IS 1
5650 PRINT Do.Dl.Kcu
5655 ASSIGN #File TO File5
5660 ENTER #File:Nrun.Date5.Ldte1.Ldte2.Ist
5665 Ru=Do*LOG(Do/D1)/(2*Kcu)
5670 Sx=0
5675 Sy=0
5680 Sxv=0
5685 Sx2=0
5690 Sv2=0
5695 FOR I=1 TO Nrun
5700 ENTER #File:Bop.Tdts.Emf(*).Fms
5705! CONVERT EMF TO TEMPERATURE
5710 FOR J=1 TO 5
5715 T(J)=FHTvsV(Emf(J))
5720 NEXT J
5725 Tbat=(T(1)+T(2))+.15
5730 Tavg=(5)

```



```

5735 Grad=17.9855+.114188*Tavg
5740 Tdrop=Tm*(7)+1.E-6*(10)+Grad
5745 Tavgc=T(S)-Tdrop*.5
5750 IF ABS(Tavg-Tavgc)>.01 THEN
5755 Tavg=(Tavg+Tavgc)*.5
5760 GOTO 5735
5765 END IF
5770!
5775! Compute properties of water
5780 Kw=FNKw(Tavg)
5785 Muw=FNMuw(Tavg)
5790 Cpw=FNCPw(Tavg)
5795 Pw=FNPPw(Tavg)
5800 Rhow=FNRRow(Tavg)
5805!
5810! Compute properties of Freon-114
5815 Lmtd=Tdrop/LOG((T(S)-Tsat)/(T(S)-Tdrop-Tsat))
5820 IF J1=0 THEN
5825 Tw=Tsat+Fre*Lmtd
5830 Thetad=Tw-Tsat
5835 J1=1
5840 END IF
5845 Tf=(Tw+Tsat)*.5
5850 Rho=FNRRho(Tf)
5855 Mu=FNMu(Tf)
5860 K=FNK(Tf)
5865 Cp=FNCP(Tf)
5870 Beta=FNBeta(Tf)
5875 Hfg=FNHfg(Tsat)
5880 N1=Mu/Rho
5885 Alpha=K/(Rho*Cp)
5890 Pr=N1/Alpha
5895!
5900! Analysis
5905! COMPUTE MDDT
5910 A=PI*(Do2-Di2)/4
5915 P=PI*Do
5920 Mdot=3.9657E-3+Fms*(3.51955E-3-Fms*(8.32006E-6-Fms*(1.23638E-7-Fms*4.31897E-10)))
5925 Q=Mdot*Cpw*Tdrop
5930! COMPUTE NATURAL-CONVECTIVE HEAT-TRANSFER COEFFICIENT
5935! FOR UNENHANCED ENDS(2)
5940 Hbar=190
5945 Fe=(Hbar*P/(Kcu*A))*.5*Lu
5950 Tann=FNNTann(Fe)
5955 Theta=Thetad*Tann/Fe
5960 X=(9.31+Beta*Theta+Do3*Tann/(Fe*N1*Alpha))*.166667
5965 Yy=(1+(.559/Pr)1/4*(9/16))1/4*(8/27)
5970 Hbarc=X/Do*(.5+.387*X/Yy)1/2
5975 IF ABS((Hbar-Hbarc)/Hbar)>.001 THEN
5980 Hbar=(Hbar+Hbarc)*.5
5985 GOTO 5945
5990 END IF
5995!
6000! COMPUTE HEAT LOSS RATE THROUGH UNENHANCED ENDS
6005 Q1=(Hbar*P*xcu*A)*.5*Theta*Tann
6010 Qc=Q1-Q1
6015 As=PI*Do*L
6020! COMPUTE ACTUAL HEAT FLUX
6025 Qdp=Qc/As

```

```

7030 IF Icfl.x=1 OR Icfl.x=2 THEN Uo=1/CF*(1/Rr)
7035 Thetad=CsF/Do+Hfg+(Qdp/(Mu+Hfg)+(1/4)*(9.81+Rho))*(E*(1/Rr)+Rr)
7040 Ho=Qdp/Thetad
7045 Omega=Ho/CF
7050 Uo=U/(PI*Do*L*Lmda)
7055 Vu=Mdot/(Rhow*PI*Di^2/4)
7060 Rew=Rhow*Vu*Di/Muwa
7065 Twl=Tw+Q*Rw/(PI*Do*L)
7070 Gama=Xw/Di+Rew*.3*Prw*(1/3.)*(Muwa/FHMuw(Twl))^1.14
7075! PRINTER IS
7080 Yw=(1./Uo-Rw)*Omega
7085 Xw=Omega*Do/(Gama*Di)
7090 Sx=Sx+Xw
7095 Sy=Sy+Yw
7100 Sxy=Sxy+Yw*Xw
7105 Sx2=Sx2+Xw*Xw
7110 Sy2=Sy2+Yw*Yw
7115 NEXT I
7120 ASSIGN #File TO *
7125 M=(Sx*Sy-Nrun*Sxy)/(Sx*Sx-Nrun*Sx2)
7130 C=(Sy-Sx*M)/Nrun
7135 IF Icfl.x=0 OR Icfl.x=3 OR Icfl.x=4 THEN
7140 C1=1/M
7145 C1c=1/C
7150 END IF
7155 IF Icfl.x=1 THEN
7160 C1c=1/M
7165 C1c=C1
7170 END IF
7175 IF Icfl.x=2 THEN
7180 C1c=0.1
7185 C1c=1/C
7190 END IF
7195 IF Icfl.x=3 THEN 7080
7200 IF ABS((C1-C1c)/C1c)>.10 OR ABS((C1-C1c)/C1c)>.001 THEN
7205 C1=(C1+C1c)*.5
7210 C1c=(C1c+C1c)*.5
7215 PRINTER IS
7220 PRINT USING "2X, "" Csf = "" .MZ.3DE.2X, "" C1 = "" .MZ.3DE":Csf,C1
7225 PRINTER IS
7230 GOTO 5655
7235 END IF
7240 PRINT
7245 PRINTER IS "0"
7250 PRINT USING "2X, "" C1 "" "" C1 "" ""
7255 PRINT USING "3X, "" ASSUMED "" "" .MZ.3DE.3X.MZ.3DE":C1a,C1a
7260 PRINT USING "3X, "" CALCULATED "" "" .MZ.3DE.3X.MZ.3DE":Csf,C1
7265 PRINT
7270 Sum2=Sy2+2*M*Sxy+2*C*Sy+M^2*Sx2+2*M*C*Sx+Nrun*C^2
7275 PRINT USING "10X, "" Sum of Squares = "" .Z.3DE":Sum2
7280 PRINT USING "10X, "" Coefficient = "" .D.3DE":Rr
7285 SUBEND
7290 DEF FNMuw(T)
7295 A=247.3/(T+100.15)
7298 Mu=3.4E-5+10*A
7300 RETURN Mu
7305 FNEND
7310 DEF FNCsf(T)
7315 Csf=4.1E-1085A-T*(1.25825E-11-T*(4.42261E-15+2.77423E-17*T))
7320 RETURN Csf
7325 FNEND

```

```

7030 DEF FNRoww(T)
7035 Ro=999.62046-T*(.01063-T*(5.48251DE-3-T*(1.234147E-5)))
7040 RETURN Ro
7045 FNEND
7050 DEF FNPpw(T)
7055 Ppw=FNRoww(T)+FNMmw(T)/FNKw(T)
7060 RETURN Ppw
7065 FNEND
7070 DEF FNKw(T)
7075 X=(T+273.15)/273.15
7080 Kw=-.92247+X*(2.3395-X*(1.3007-X*(.52577-.07344*X)))
7085 RETURN Kw
7090 FNEND

```

```

10065 SUB Select
10070 COM /Idp/ Idp
10075 BEEP
10080 PRINTER IS :
10085 PRINT USING "4X.";"Select option:"
10090 PRINT USING "5X.";"0 Taking data or re-processing previous data"
10095 PRINT USING "5X.";"1 Plotting data on Log-Log"
10400 PRINT USING "5X.";"2 Plotting data on Linear"
10405 PRINT USING "5X.";"3 Make cross-plot coefft file"
10410 PRINT USING "5X.";"4 Re-circulate water"
10415 PRINT USING "5X.";"5 Purge"
10420 PRINT USING "5X.";"6 T-Drop correction"
10425 PRINT USING "5X.";"7 Print Jo File"
10430 INPUT Idp
10435 IF Idp=0 THEN CALL Main
10440 IF Idp=1 THEN CALL Plot
10445 IF Idp=2 THEN CALL Plin
10450 IF Idp=3 THEN CALL Coef
10455 IF Idp=4 THEN CALL Main
10460 IF Idp=5 THEN CALL Purg
10465 IF Idp=6 THEN CALL Tdch
10470 IF Idp=7 THEN CALL Uoprt
10475 SUBEND

```

APPENDIX B
FLOWMETER CALIBRATION

A Fischer Porter Flowmeter was used in the experimental apparatus to indicate the water flowrate. Prior to conducting the boiling tube data runs, calibration of the flowmeter was performed over a temperature range from 19 °C to 38 °C. The goals of the calibration were:

- 1) to develop a mathematical expression relating flowmeter percent reading to mass flowrate and
- 2) to determine a viscosity correction factor due to varying temperature range and flowrates.

A weigh tank, platform-type scale, and stopwatch were used to record water collection data.

Data were processed using the program "FMCAL", listed later in this appendix. This program took the flowmeter percent reading, water weight collected, and elapsed water collection time as the inputs. The outputs were an experimental mass flowrate and a mass flowrate difference. This difference was given by a mass flowrate computed from a correlation minus the experimental mass flow rate for the same flowmeter percent reading. The correlation was based on a fourth-order least-squares fit to the calibration data. After all the data runs were completed, the data points were combined into one file and a single fourth-order polynomial was generated to describe the relationship between the flowmeter percent reading and the mass flowrate. Of the original data points, 98.61 percent were within a ± 5.5 percent range. Reprocessing the data points led to 78 percent within a ± 1.02 percent range. The equation (B.1), resulting from the calibration data analysis, is a fourth-order polynomial from a curve fit of the reprocessed data without a viscosity correction factor:

$$\dot{m} = 3.0657e-3 + 3.1690e-3(FMS) - 3.8020e-6(FMS)^2 + 1.2369e-7(FMS)^3 - 4.3100e-10(FMS)^4 \quad (B.1)$$

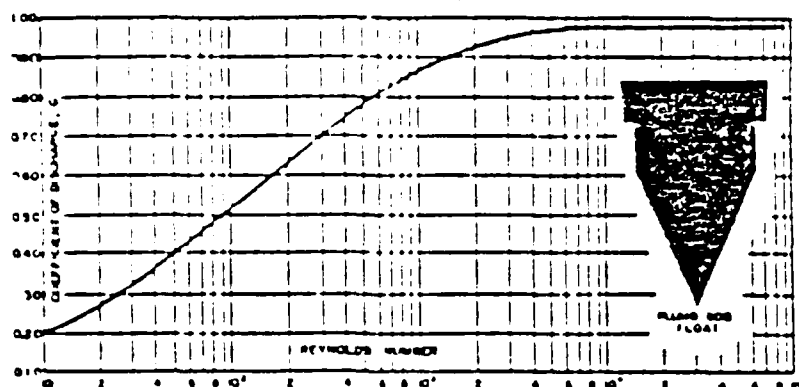
(FMS = flowmeter percent reading)

Experimental discharge rates are less than the rates calculated from theoretical flow equations primarily because of the effect of internal molecular friction of the fluid and the viscosity. The theoretical flow equation is:

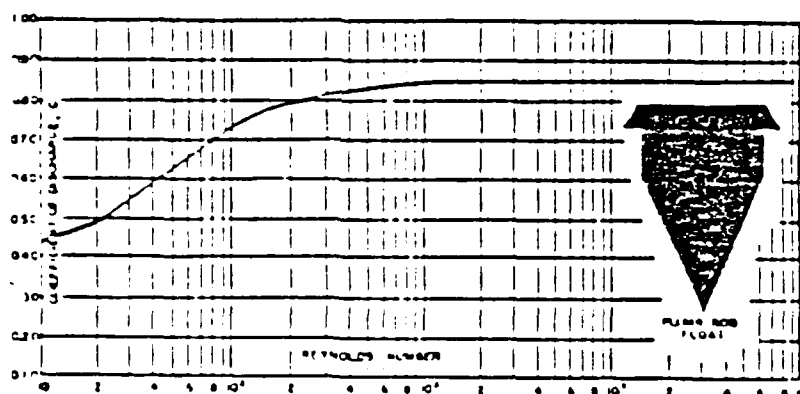
$$Q = A_w C_d \left[\frac{2gV_f(\rho_f - \rho_w)}{A_f \rho_w} \right]^{0.5} \quad (B.2)$$

where Q =volumetric flowrate, A_w =cross-sectional area of the narrowest part of annulus, V_f =volume of float, ρ_f = density of float, A_f =cross-sectional area of the largest part of float, and ρ_w =density of fluid. The Coefficient of Discharge, C_d , is a function of viscosity. A constant value for C_d in equation (B.2) would be desirable as this would show a negation in the variations due to the viscosity. The effect of the float shape on C_d with varying Reynolds number is shown in Figure B.1 (a). The Reynolds number for the flowmeter uses an effective diameter of the tube inner diameter minus the float outer diameter. This plumb bob style float presents a large surface area to the fluid stream and the viscous effects increase as the flow rate increases. [Ref. 31: pp. 9804-9808]

The data collected from the calibration runs showed little or no change in the Discharge Coefficient over the 20 to 90 percent flowmeter setting range and the 15 K change in fluid temperature. The square edge plumb bob float reaches a constant Coefficient of Discharge at Reynolds



(a)



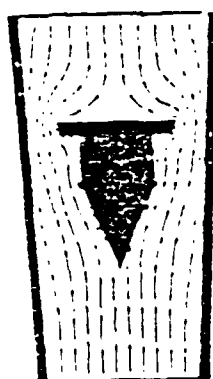
(b)

Figure B.1. Effect of Float Shape on Coefficient of Discharge: (a) Square Edge Plumb Bob Float (from Ref. 30), and (b) Taper Edge Plumb Float.

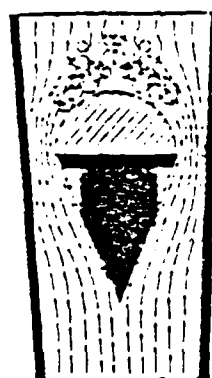
number > 10000 . This is due to the effective shape of the float on the streamline pattern as shown in Figures B.2 (a) and (b). The experimental calibration range of $1300 < Re < 27000$ displayed a flattening out of the Coefficient of Discharge. A different effective shape is seen by the streamline pattern because of the minimal clearances between the tube bead guides and the float. Also, the float used in this particular flowmeter had tapered edges versus square edges. This different effective shape is shown Figures B.2 (c) and (d). Figure B.1 (b) shows the effect of the float shape on the Coefficient of Discharge for the tapered edge float.

Additionally, the accuracy of the flowmeter contributes to the flattening effect on the Coefficient of Discharge shown by the experimental data. The accuracy effect is felt in two major components, reproducibility and scale factor. Reproducibility accuracy is minimally determined by the change in the fluid flowrate, corresponding float movement, and observation of float position. The calibration data had good reproducibility over the various flowrate and temperature ranges. The scale factor accuracy is inherent to the scale markings on the flow tube. Fischer Porter conducted numerous tests of flowmeter calibration readings. They used a maximum scale fraction error of 0.9 mm on a 250 mm tube. Based on their results, Fischer Porter reported [Ref. 31: pp. 9814-9816] an accuracy of plus or minus one percent at high flow rates was a reasonable expectation. Also, at low flow rates (< 20 percent) a reasonable expectation would be an accuracy of eight to ten percent.

The experimental data followed a trend of negligible viscosity effect. The flow tube design, float shape, and scale factor accuracy were the main contributors to this negation of a viscosity correction factor. As such, equation (B.1) was used without a viscosity correction factor to calculate the mass flowrate for the boiling tube runs.

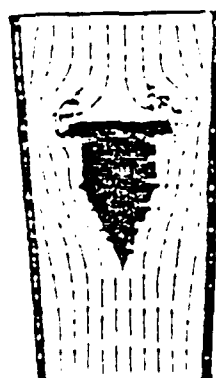


Low Velocity Flow



High Velocity Flow

(a)



Low Velocity Flow



High Velocity Flow

(b)

Figure B.2. Effect of Float Shape on Streamline Pattern:
 (a) Square Edge Plumb Bob Float (from Ref. 30),
 and (b) Taper Edge Plumb Bob Float.

APPENDIX C MODIFIED WILSON PLOT

As referenced in Chapters III and IV, this appendix provides the data reduction procedures used to compute inside and outside heat-transfer coefficients. The tubes used for data collection were the smooth, modified High Flux, and Modified Turbo-B tubes. The modified Wilson plot analysis could not be directly run on the enhanced tubes since reliable boiling correlations for these surfaces do not exist. Also, only two unknowns can be allowed between correlations for the inside and outside heat-transfer coefficients. The steps used in this procedure are outlined below and are contained in DRP4, which is cited in Appendix A:

Basic Equations

The overall heat-transfer coefficient in terms of the overall thermal resistance is given by:

$$\frac{1}{U_o} = \frac{A_o}{h_i A_i} + R_w + \frac{1}{h_o} \quad (C.1)$$

where

$$R_w = D_o \ln \left(\frac{D_o}{D_i} \right) \frac{.5}{k_m} \quad (C.2)$$

Modified Wilson Plot

1. Assume C_{sf} and T_f for the boiling side and compute:

$$\Omega = \left(\frac{C_p}{Pr^{1/3}} \right)^{1/4} \left[\frac{g(\rho_l - \rho_v)}{g_{c1} \sigma_1} \right]^{0.5} \frac{u \Delta T^2}{h_{fg}^2} \quad (C.3)$$

$$h_o = \frac{\Omega}{(C_{sf})^{1/4} r} \quad (C.4)$$

Note: with r equal to 0.333, equation (C.3) represents the Rohsenow correlation [Ref. 23: p. 969].

2. Assume C_i and compute:

$$\Gamma = \frac{k}{D_i} Re^{0.8} Pr^{0.33} \left(\frac{u}{u_w} \right)^{0.14} \quad (C.5)$$

$$h_i = C_i \Gamma \quad (C.6)$$

3. Substitute h_o and h_i from steps 1 and 2 above into equation (C.1) and rearrange to yield:

$$\frac{1}{U_o} - R_w \Omega = \frac{A_o \Omega}{C_i A_i \Gamma} + (C_{sf})^{1/4} \quad (C.7)$$

4. Now, let:

$$Y = \frac{1}{U_o} - R_w \Omega \quad (C.8)$$

and

$$X = \frac{A_o \Omega}{A_i \Gamma} \quad (C.9)$$

Construct the least-squares line for Y versus X in the form of:

$$Y = mX + C \quad (C.10)$$

5. Compute a new set of values for C_i and C_{sf} as follows:

$$C_i = \frac{1}{m} \quad (C.11)$$

and

$$C_{sf} = C^r \quad (C.12)$$

6. Repeat steps 1 through 5 until convergence for C_i and C_{sf} between two successive iterations is less than 0.1 percent.

APPENDIX D

DATA RUNS

The following table outlines the data runs used in this investigation:

Where:

1. WH - Smooth tube
2. HF- High Flux (i.e., porous-coated Korodense) tube
3. HFM - Modified High Flux (i.e., porous coating machined off) tube
4. TB - Turbo-B tube
5. TBM - Modified Turbo-B (i.e., external enhancement machined off) tube
6. T - inlet water temperature
7. V - water velocity
8. const - constant
9. dec - decreasing
10. inc - increasing

TABLE 4
DATA RUN DESCRIPTION

File Name	Oil %	# points	Description
WH01	0	10	Light Off Effect (cold water)
WH02	0	10	Light Off Effect (warm water)
WH03	0	9	Light Off Effect (steam)
WH05	0	10	T const V dec
WH06	0	8	T const V dec
WH07	1	10	T const V dec
WH08	1	10	T const V dec
WH09	2	10	T const V dec
WH10	2	10	T const V dec
WH10A	2	10	Repeatability WH10
WH11	6	10	T const V dec
WH12	6	8	T const V dec
WH13	6	8	Light Off Effect (warm water)
HF12	0	10	T const V dec
HF13	0	12	T const V dec Light Off Effect (steam)
HF14	0	12	Light Off Effect (cold water)
HF15	0	10	Light Off Effect (warm water)
HF16	0	12	Repeatability of HF12
HF22	0	7	T inc V const
HF23	0	6	T dec V const
HF24	1	12	T const V dec
HF25	1	10	T const V dec
HF26	1	6	T dec V const
HF27	1	7	T inc V const
HF28	2	12	T const V dec
HF29	2	12	T const V dec
HF30	2	6	T dec V const (Repeatability of HF28)
HF31	2	8	T inc V const
HF32	6	10	T const V dec
HF33	6	10	T const V dec
HF34	6	7	T dec V const
HF35	6	7	T inc V const
HFM01	0	8	Sieder-Tate Coeff Run
HFM02	0	8	Sieder-Tate Coeff Run
HFM03	0	10	Sieder-Tate Coeff Run
HFM04	0	8	Sieder-Tate Coeff Run
HFM05	0	8	Sieder-Tate Coeff Run
HFM06	0	8	Sieder-Tate Coeff Run
HFM07	0	10	Sieder-Tate Coeff Run
HFM08	0	8	Sieder-Tate Coeff Run
TB01	0	10	Light Off Effect (cold water)
TB02	0	10	Light Off Effect (warm water)
T303	0	10	Light Off Effect (steam)

TB04	0	10	T	const	V	dec	
			(Repeatability of TB03)				
TB05	0	6	T	dec	V	const	
TB06	0	10	T	const	V	dec	
TB07	0	7	T	inc	V	const	
TB08	1	10	T	const	V	dec	
TB09	1	6	T	dec	V	const	
TB10	1	10	T	const	V	dec	
TB11	1	6	T	inc	V	const	
TB12	2	10	T	const	V	dec	
TB13	2	10	T	const	V	dec	
			(Repeatability of TB12)				
TB14	2	7	T	dec	V	const	
TB15	2	10	T	const	V	dec	
TB16	2	6	T	inc	V	const	
TB17	6	10	T	const	V	dec	
TB18	6	7	T	dec	V	const	
TB19	6	7	T	inc	V	const	
TB20	6	8	T	const	V	dec	
			Light Off Effect				
			(steam)				
TB21	6	10	Light Off Effect				
			(cold water)				
TB22	6	10	Light Off Effect				
			(warm water)				
TBM04	0	8	Sieder-Tate	Coeff		Run	
TBM05	0	8	Sieder-Tate	Coeff		Run	
TBM06	0	6	Sieder-Tate	Coeff		Run	
TBM07	0	6	Sieder-Tate	Coeff		Run	
TBM08	0	8	Sieder-Tate	Coeff		Run	
TBM09	0	8	Sieder-Tate	Coeff		Run	
TBM10	0	8	Sieder-Tate	Coeff		Run	

APPENDIX E

UNCERTAINTY ANALYSIS

The uncertainty for mass flow rate, Reynolds number, heat flux, LMTD, wall resistance, overall heat-transfer coefficient, inside heat-transfer coefficient, and outside heat-transfer coefficient were analyzed for selected runs of the smooth, High Flux and Turbo-B tubes. The analysis was based on the Kline-McClintock [Ref. 32: p. 3] method of uncertainty analysis. For example, the following equations were used for the uncertainty of the heat flux:

$$q = \frac{Q}{\pi D_o L} \quad (E.1)$$

and

$$Q = \dot{m} c_p (\bar{T}_{in} - \bar{T}_{out}) \quad (E.2)$$

In accordance with Kline and McClintock, the uncertainties are given by:

$$\frac{\delta q}{q} = \left[\left(\frac{\delta Q}{Q} \right)^2 + \left(\frac{\delta D_o}{D_o} \right)^2 + \left(\frac{\delta L}{L} \right)^2 \right]^{0.5} \quad (E.3)$$

and

$$\frac{\delta Q}{Q} = \left[\left(\frac{\delta \dot{m}}{\dot{m}} \right)^2 + \left(\frac{\delta c_p}{c_p} \right)^2 + \left(\frac{\delta \bar{T}_{in}}{(\bar{T}_{in} - \bar{T}_{out})} \right)^2 + \left(\frac{\delta \bar{T}_{out}}{(\bar{T}_{in} - \bar{T}_{out})} \right)^2 \right]^{0.5} \quad (E.4)$$

The uncertainty in the conduction losses for the unenhanced ends of the boiling tube were considered negligible in comparison to the boiling surface uncertainty and as such, were disregarded. Table 5 lists the uncertainties for the previously mentioned values.

TABLE 5
UNCERTAINTY ANALYSIS PERCENTS

file	WH05	WH05	HF13	HF13	TB04	TB04
q	31140	26690	49540	38780	68780	53670
(w/m)						
$\frac{q}{V}$	2.24	1.39	2.24	1.39	1.37	1.07
(m/s)						
$\frac{\delta q}{q}$	1.56	2.51	1.56	2.51	1.43	2.51
$\frac{\delta Re}{Re}$	1.79	2.65	1.73	2.61	1.61	2.61
$\frac{\delta q}{q}$	1.59	2.52	1.59	2.52	1.46	2.52
$\frac{\delta LMTD}{LMTD}$	4.96	3.59	3.10	2.45	2.29	1.66
$\frac{\delta R_w}{R_w}$	2.76	2.76	11.17	11.17	2.92	2.92
$\frac{\delta U_o}{U_o}$	5.21	4.39	3.48	3.52	2.71	3.02
$\frac{\delta h_1}{h_1}$	2.03	2.56	1.61	2.25	1.48	2.21
$\frac{\delta h_2}{h_2}$	5.34	5.08	4.90	4.89	3.35	3.96

Note: All runs were performed in pure refrigerant
 WH = Smooth tube
 HF = Korodense tube with High Flux Coating
 TB = Turbo-B tube

The large uncertainty for the wall resistance of file HF13 (porous-coated Korodense tube) is due to the 10 percent uncertainty of the thermal conductivity coefficient. For this investigation, the coefficient used was an average value for the values given in the open literature for copper-nickel plates or tubes.

APPENDIX F
LIST OF NOMENCLATURE

1. NOMENCLATURE

A - Surface Area
 c_p - Specific heat at constant pressure
 C_o - Oil concentration
 C_i - Inside Sieder-Tate-type coefficient
 C_{sf} - Rohsenow coefficient
 d_i - Inside diameter of tube
 d_o - Diameter of mouth of reentrant cavity
D - Diameter
e - Depth of internal ridge or fin
 E_v - Energy transfer per unit volume
f - Friction factor
g - Acceleration due to gravity
 g_c - Gravitational constant
h - Convective heat-transfer coefficient
 h_{fg} - Specific enthalpy of vapor-liquid mixture
k - Conductive heat-transfer coefficient
 k_m - Conductive heat-transfer coefficient of metal
L - Tube length
 L_e - Entrance effect length
 \dot{m} - Mass flow rate
p - Distance between ridge or fin peaks
Pr - Prandtl number
q - Heat flux
Q - Total heat transfer
r - Tube radius
Re - Reynolds number
 R_w - Thermal wall resistance
St - Stanton number

U_o - Overall heat-transfer coefficient
 v_g - Specific volume of vapor
 V - Velocity
 Δ - Change (i.e., $T_{in} - T_{out}$)
 σ - Surface tension
 σ_o - Surface tension of oil
 σ_r - Surface tension of refrigerant
 μ - Viscosity
 μ_o - Viscosity of oil
 μ_r - Viscosity of refrigerant
 ρ - Density
 ρ_o - Density of oil
 ρ_r - Density of refrigerant

2. SUBSCRIPTS

f - fluid
i - inside
in - inlet
m - mixture
o - outside
ol - oil-liquid
out - outlet
rl - refrigerant-liquid
s - smooth tube
sat - saturation
w - water
wo - outside wall

AD-A175 246

NUCLEATE POOL-BOILING OF R-114 REFRIGERANT AND OIL
MIXTURES FROM WATER-HEATED ENHANCED SURFACES(U) NAVAL
POSTGRADUATE SCHOOL MONTEREY CA 5 N MCMAHUS JUN 86

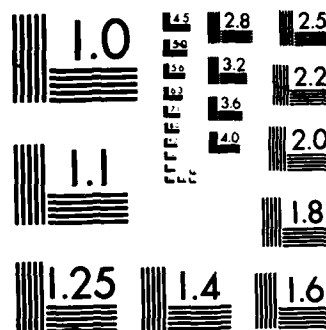
2/2

UNCLASSIFIED

F/G 28/13

NL





XERO COPY RESOLUTION TEST CHART

LIST OF REFERENCES

1. Bergles, A. E. and Webb, R. L., "A Guide To The Literature on Convective Heat Transfer Augmentation," Advances in Enhanced Heat Transfer, Vol. 43, pp. 81-89, 1985.
2. Wanniarachchi, A. S., Marto, P. J., and Reilly, J.T., "The Effect of Oil Contamination on the Nucleate Pool-Boiling Performance of R-114 from a Porous-Coated Surface," ASHRAE Transactions, pp. 2-73, 1986 (accepted for publication).
3. ASHRAE Guide and Data Book, Chapter 18, pp. 281-291, 1963.
4. Dougherty, R. L. and Sauer, Jr., H. J., "Nucleate Pool Boiling of Refrigerant-Oil Mixtures From Tubes," ASHRAE Transactions, Vol. 80, pp. 175-178, 1975.
5. Chongrungleong, S. and Sauer Jr., H. J., "Nucleate Boiling Performance of Refrigerants and Refrigerant-Oil Mixtures," ASME Transactions, Vol. 102, pp. 701-705, November, 1980.
6. Fujii, M., Nishiyama, E., and Yamanaka, G., "Nucleate Pool Boiling Heat Transfer From Micro-Porous Heating Surfaces," Advances in Enhanced Heat Transfer, pp. 45-50, 1979.
7. Webb, R. L., "The Evolution of Enhanced Surface Geometries for Nucleate Boiling," Heat Transfer Engineering, Vol. 2, nos 3-4, pp. 46-69, Jan-June, 1981.
8. Reilly, J. T., The Influence of Oil Contamination on the Nucleate Pool-Boiling Behavior of R-114 from a Structured Surface, M. S. Thesis, Naval Postgraduate School, Monterey, California, pp. 30-35, 65, 70, March, 1985.
9. Czikk, A. M. and O'Neill, P. S., "Correlation of Nucleate Boiling From Porous Metal Films," Advances in Enhanced Heat Transfer, pp. 53-59, 1979.
10. Carnavos, T. C., "An Experimental Study: Pool Boiling R-11 With Augmented Tubes," Advances in Enhanced Heat Transfer, pp. 103-108, 1981.
11. Czikk, A. M., Gottzmann, C. F., Ragi, E. G., Withers, J. G., and Haddas, E. P., "Performance of Advanced Heat Transfer Tubes in Refrigerant-Flooded Liquid Coolers," ASHRAE Transactions, Vol. 76, part 1, pp. 96-107, 1970.

12. Arshad, J. and Thome, J. R., "Enhanced Boiling Surfaces: Heat Transfer Mechanism Mixture Boiling," ASME-JSME Thermal Energy Engineering Joint Conf., Vol. 1, pp. 191-197, 1983.
13. Arai, N., Nakajima, T., Fukushima, T., Fujie, K., Arai, A., and Nakayama, Y., "Heat Transfer Tubes Enhancing Boiling and Condensation in Heat Exchangers of a Refrigerating Machine," ASHRAE Transactions, Vol. 83, part 2, pp. 58-62, 1977.
14. Ayub, Z. H. and Bergles, A. E., "Pool Boiling from Grew Surfaces in Water and R-113," Augmentation of Heat Transfer in Energy Systems, Vol. 52, pp. 57-64, 1985.
15. Nakayama, W., Daikoku, T., Kuwahara, H., and Nakajima, T., "Dynamic Model of Enhanced Boiling Heat Transfer on Porous Surfaces," Advances in Enhanced Heat Transfer, pp. 31-43, 1979.
16. Jensen, M. K. and Jackman, D. L., "Prediction of Nucleate Pool Boiling Heat Transfer Coefficients of Refrigerant-Oil Mixtures," ASME Transactions, Vol. 106, pp. 184-190, 1984.
17. Marto, P. J., Reilly, D. J., and Fenner, J. H., "An Experimental Comparison of Enhanced Heat Transfer Condenser Tubing," Advances in Enhanced Heat Transfer, pp. 1-8, 1979.
18. GA Technologies Report, GA-A17833, Fluid Mechanics and Heat Transfer Spiral Fluted Tubing, by J. S. Yampolsky et. al., 1984.
19. DSR Report, 70790-69, Investigation of Heat Transfer Augmentation Through Use of Internally Finned and Roughened Tubes, by A. E. Bergles et. al., pp. 18-23, 1970.
20. Karasbun, M., An Experimental Apparatus to Study Nucleate Pool Boiling of R-114 and Oil Mixtures, M. S. Thesis, Naval Postgraduate School, Monterey, California, pp. 24-32, 54-56, December, 1984.
21. Chaddock, J. B., "Influence of Oil Refrigerant Evaporator Performance," ASHRAE Transactions, Vol. 82, part 1, pp. 474-486, 1976.
22. AERE Report, R7318, The Development of Heat Transfer Tubes, by I. H. Newson and T. D. Hudson, 1973.
23. Rohsenow, W. M., "A Method of Correlating Heat Transfer Data for Surface Boiling of Liquids," ASME Transactions, Vol. 74, p. 969, 1952.

24. Incropera, F. P. and DeWitt, D. P., Fundamentals of Heat Transfer, John Wiley and Sons, p. 406, 1981.
25. Withers, J.G., "Tube-side Heat Transfer and Pressure Drop for Tubes Having Internal Helical Ridging with Turbulent/Transitional Flow of Single-phase Fluid: Part 1--Single-helix Ridging," Heat Transfer Engineering, Vol 2, No. 2, 1980.
26. Withers, J. G., "Tube-side Heat Transfer and Pressure Drop for Tubes Having Internal Helical Ridging with Turbulent/Transitional Flow of Single-phase Fluid: Part 2--Multiple-helix Ridging," Heat Transfer Engineering, Vol 2, No. 2, 1980.
27. Nobukatsu, A. and et. al., "Heat Transfer Tubes Enhancing Boiling and Condensation in Heat Exchangers of a Refrigerating Machine," ASHRAE Transactions, Vol. 83, part 2, pp. 58-70, 1977.
28. Green, G. H., "Influence of Oil on Boiling Heat Transfer and Pressure Drop in Refrigerants 12 and 22," ASHRAE Journal, pp. 57-61, 1982.
29. Stephan, K., "Influence of Oil on Heat Transfer of Boiling Freon 12 (Refrigerant 12) and Freon 22 (Refrigerant 22)," Proceedings of XIth International Congress of Refrigeration, Vol. 1, pp. 369-379, 1963.
30. Stephan, K., and Mitrovic, J., "Heat Transfer in Natural Convection Boiling of Refrigerant-Oil Mixtures," Models and Correlations Review, pp. 73-85, 1982.
31. Fischer and Porter Company, Theory of the Flowrator, Catalog Section 98-A, pp. 9801-9816, 1947.
32. Kline, S. J. and McClintock, F. A., "Describing Uncertainties in Single-Sample Experiments," Mechanical Engineering, p. 3, Jan. 1953.

INITIAL DISTRIBUTION LIST

	No.	Copies
1. Library Code 0142 Naval Postgraduate School Monterey, California 93943		2
2. Defense Technical Information Center Cameron Station Alexandria, Virginia 22314-6145		2
3. Department Chairman, Code 69 Department of Mechanical Engineering Naval Postgraduate School Monterey, California 93943		1
4. Professor Paul J. Marto, Code 69 Mx Department of Mechanical Engineering Naval Postgraduate School Monterey, California 93943		3
5. Dr. A. S. Wanniarachchi, Code 69Wa Department of Mechanical Engineering Naval Postgraduate School Monterey, California 93943		2
6. Dr. B. H. Hwang, Code 2722V David W. Taylor Naval Ship Research and Development Center Annapolis, Maryland 21402		1
7. Mr. R. Helmick, Code 2745 David W. Taylor Naval Ship Research and Development Center Annapolis, Maryland 21402		1
8. Mr. N. R. Clevinger Product and Process Development Mgr. Wolverine Tube P. O. Box 2202 Decatur, Alabama 35602		1
9. Mr. J. McManus Box 139 Logan Lake, British Columbia Canada V0K 1W0		1
10. Lt. S. McManus 6840 N. Columbus Blvd Tucson, Arizona 85718		2
11. Mr. Elias Ragi Union Carbide Corporation P. O. Box 44 Tonawanda, New York 14151		1
12. Dr. Masafumi Katsuta School of Science and Engineering 3-4-1, Ohkubo, Shinjukuku, Tokyo, 160, Japan		1

AN-7175-246

REPORT DOCUMENTATION PAGE

1a REPORT SECURITY CLASSIFICATION UNCLASSIFIED			1b. RESTRICTIVE MARKINGS	
2a SECURITY CLASSIFICATION AUTHORITY			3 DISTRIBUTION/AVAILABILITY OF REPORT Approved for public release; distribution unlimited.	
2b DECLASSIFICATION/DOWNGRADING SCHEDULE			5 MONITORING ORGANIZATION REPORT NUMBER(S)	
3 PERFORMING ORGANIZATION REPORT NUMBER(S)			5 MONITORING ORGANIZATION REPORT NUMBER(S)	
6a NAME OF PERFORMING ORGANIZATION Naval Postgraduate School		6b OFFICE SYMBOL (If applicable) Code 69		7a. NAME OF MONITORING ORGANIZATION Naval Postgraduate School
6c ADDRESS (City, State, and ZIP Code) Monterey, California 93943-5000			7b. ADDRESS (City, State, and ZIP Code) Monterey, California 93943-5000	
8a NAME OF FUNDING/SPONSORING ORGANIZATION David W. Taylor NSRDC		8b OFFICE SYMBOL (If applicable)		9 PROCUREMENT INSTRUMENT IDENTIFICATION NUMBER
8c ADDRESS (City, State, and ZIP Code) Annapolis, Maryland 21402			10 SOURCE OF FUNDING NUMBERS	
			PROGRAM ELEMENT NO	PROJECT NO
			TASK NO	WORK UNIT ACCESSION NO
11 TITLE (Include Security Classification) Nucleate Pool-Boiling of R-114 Refrigerant and Oil Mixtures from Water-Heated Enhanced Surfaces				
12 PERSONAL AUTHOR(S) McManus, Stephen, M.				
13a TYPE OF REPORT Master's Thesis		13b TIME COVERED FROM TO		14 DATE OF REPORT (Year, Month, Day) 1986, June
15 PAGE COUNT 99				
16 SUPPLEMENTARY NOTATION				
17 COSATI CODES			18 SUBJECT TERMS (Continue on reverse if necessary and identify by block number)	
FIELD	GROUP	SUB-GROUP	Nucleate Pool-Boiling; Water-Heated Tubes; Enhanced Surfaces; <i>Energy; Computer Programs, C</i>	
19 ABSTRACT (Continue on reverse if necessary and identify by block number) Heat-transfer measurements were made for a single, water-heated tube in a pool of R-114 to simulate operating conditions of a water chiller. Data were obtained for a smooth copper tube, and for two commercially available tubes: a spirally roped copper-nickel tube with a porous coating; and a copper tube with a structured outer surface and a multiple-start helical ridged inner surface. Measurements were made for refrigerant-oil mixtures at oil concentrations from 0 to 6 mass percent with a boiling pool temperature of 13.8 °C. Results for the two enhanced tubes with and without oil are compared to the smooth tube data. Enhancement factors for the overall heat-transfer coefficient were 4.0 and 3.6 for the structured surface and porous-coated tubes, respectively, in pure refrigerant and at a water velocity of 2 m/s. For these same conditions the enhancement factors (cont. next page)				
20 DISTRIBUTION STATEMENT OF ABSTRACT <input checked="" type="checkbox"/> UNCLASSIFIED UNLIMITED <input type="checkbox"/> SAME AS RPT <input type="checkbox"/> DTIC USERS			21 ABSTRACT SECURITY CLASSIFICATION Unclassified	
22a NAME OF RESPONSIBLE INDIVIDUAL P.J. Marto			22b TELEPHONE (Include Area Code) (408) 646-2586	
			22c OFFICE SYMBOL 69 MX	

Unclassified

SECURITY CLASSIFICATION OF THIS PAGE (When Data Entered)

19. (cont)
for the out-side heat-transfer coefficient were 14.6 and 6.4 for
the porous-coated and structured surface tubes, respectively.

14-0102-15-014-6601

Unclassified

SECURITY CLASSIFICATION OF THIS PAGE (When Data Entered)

Approved for public release; distribution is unlimited.

Nucleate Pool-Boiling
of R-114 Refrigerant and Oil Mixtures
from Water-Heated Enhanced Surfaces

by

Stephen M. McManus
Lieutenant, United States Navy
B. S. Ch. E., University of New Mexico, 1979

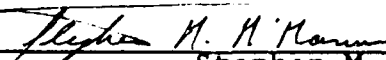
Submitted in partial fulfillment of the
requirements for the degree of

MASTER OF SCIENCE IN MECHANICAL ENGINEERING


from the

NAVAL POSTGRADUATE SCHOOL
June 1986

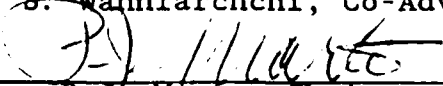
Author:

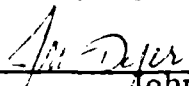

Stephen M. McManus

Approved by:


P.J. Marto, Thesis Advisor


A. S. Wanniarachchi, Co-Advisor


P.J. Marto, Chairman,
Department of Mechanical Engineering


John N. Dyer,
Dean of Science and Engineering

ABSTRACT

Heat-transfer measurements were made for a single, water-heated tube in a pool of R-114 to simulate operating conditions of a water chiller. Data were obtained for a smooth copper tube, and for two commercially available tubes: a spirally roped copper-nickel tube with a porous coating; and a copper tube with a structured outer surface and a multiple-start helical ridged inner surface. Measurements were made for refrigerant-oil mixtures at oil concentrations from 0 to 6 mass percent with a boiling pool temperature of 13.8 °C. Results for the two enhanced tubes with and without oil are compared to the smooth tube data. Enhancement factors for the overall heat-transfer coefficient were 4.0 and 3.6 for the structured surface and porous-coated tubes, respectively, in pure refrigerant and at a water velocity of 2 m/s. For these same conditions the enhancement factors for the outside heat-transfer coefficient were 14.6 and 6.4 for the porous-coated and structured surface tubes, respectively.

END

2-87

DTIC